Performance evaluation of proprietary drainage components and sheathing membranes when subjected to climate loads, task 6: hygrothermal performance of NBC-Compliant reference walls for selected Canadian locations

Saber, Hamed H.; Lacasse, Michael A.

Client Report (National Research Council of Canada. Construction), 2015-06-30

NRC·CNRC CONSTRUCTION

Performance Evaluation of Proprietary Drainage Components and Sheathing Membranes when Subjected to Climate Loads

Task 6 — Hygrothermal Performance of NBC-Compliant Reference Walls for Selected Canadian Locations

Hamed H. Saber and Michael A. Lacasse

30 June, 2015

National Research Council Canada
Conseil national de recherches Canada

Canada

Table of Contents

Table of Contents i
List of Figures iii
List of Tables v
Acknowledgements vii
Summary ix
Nomenclature xi
1.0 Background and Introduction 1
2.0 Overview of Hygrothermal Simulation Model, hygIRC-C 2
2.1 Governing Equations 2
2.1.1 Air transport - Continuity and momentum 3
2.1.2 Heat Transfer 5
2.1.3 Moisture Transfer 6
2.2 Hygrothermal Simulation Model Validation 6
3.0 Description of Wall Assemblies & Hygrothermal Property Characterization 7
3.1. Description of Wall Assemblies (Task 1) 7
3.1.1 Reference Wall Assembly 7
3.1.2 Client Wall Assemblies 9
3.2 Task 2 (Hygrothermal Property Characterization) 11
3.3 Defining Climate Loads on Wall Assembly & Drainage Systems (Task 5) 12
3.3.1 Climate loads for testing wall configurations 12
3.3.2 Weather data for hygrothermal simulation 15
3.4 Response of Wall Assemblies & Drainage Systems to Climate Loads (Task 5) 18
3.4.1. From climate loads to wind-driven rain loads acting on wall assembly and cladding 18
3.4.2 Water entry behind cladding due to permeation of cladding and deficiencies 18
3.4.3 Water retention in respective drainage systems 21
3.4.4 Moisture loads in drainage cavity at given storey heights 23
3.4.5 Distribution of moisture loads within drainage cavity 24
3.4.6 Other assumptions in respect to undertaking of hygrothermal simulations 25
Initial Conditions 25

4.0 Defining Performance Attributes 25
4.1 Locations of interest in assessing performance of wall assemblies 25
4.2 Performance criteria 27
4.2.1 RHT index 27
4.2.2 Mould index 28
4.2.3 Comparison of RHT index to Mould index 29
5.0 Results Derived from Hygrothermal Simulation 31
5.1 Comparison of simulation results over 4 storeys (Tofino, MI = 3.4) 31
5.2 Reference wall simulation - Mould index performance 32
5.2.1 Comparison in mould index response amongst different locations within wall 32
5.2.2 Comparison in mould index response within wall for selected climate locations 34
Mould index values for 1 mm "Sliver" (Figure 24) 34
Mould index for the "Back" 10 mm portion of OSB panel (Figure 25) 34
Mould index for the "Whole" 11 mm portion of OSB panel (Figure 26) 37
Mould index for interface between OSB panel and fibrous insulation(Figure 27) 37
5.2 Results for Reference Wall Simulation - RHT index performance 37
5.3 Discussion of Simulation Results 38
Response of the reference wall to different climate locations 38
Variation in values of M_{IDX} as relate to location within wall section 39
6.0 Conclusions 39

Appendix 1 – List of Task Reports 40
Appendix 2 – Hourly WDR intensity for selected Canadian locations 41
Appendix 3 – Water entry correlations - Calculated percentages as compared to measured values 42
Appendix 4 – Simulation results for Reference wall when assuming a Medium Resistant mould growth sensitivity class for wood 43

List of Figures

Figure 1 – Dependence of airflow ratio, $\boldsymbol{\Psi Flow}$, on Darcy number, $\boldsymbol{DN}$ [] 4
Figure 2– Schematic illustrating a Representative Elementary Volume (REV) in porous media [] 5
Figure 3 – West and East coast solutions for stucco installation with capillary break 8
Figure 4 – NBC code-compliant reference wall - Horizontal cross section 9
Figure 5 – Distribution of locations having MI > 1 13
Figure 6 – Maximum and 50-year return WDR in L/h (a) and L/min (b) for Canadian locations 14
Figure 7 – Maximum and 50-year return DRWP in Pa for Canadian locations 14
Figure 8 – Directional average yearly WDR intensity for (a) St. John's, NL, (b) Vancouver and (c) Tofino, BC, showing prevailing direction of maximum WDR intensity 16
Figure 9– Average WDR intensity; Cumulative Total WDR; Number of rain events; Average outdoor RH (%) over 2 years (AVG & WET year) for Vancouver, St. John's and Tofino 17
Figure 10 – Schematic illustrating WDR and DRWP loads acting on the cladding to bring about water penetration within and water entry behind the cladding 19
Figure 11 – Stucco cladding subjected to water penetration tests 20
Figure 12 – Water entry correlations for entry from (i) permeation of stucco cladding and (ii) deficiencies at through-wall penetrations 21
Figure 13 – Samples for Drainage Gap Analysis; lines on specimens show locations where specimens were sectioned horizontally and vertically 22
Figure 14 – Driange-retention test results for reference and all Client drainage systems 23
Figure 15 - Distribution of moisture loads within drainage cavities: (a) for cavities having a nominal 10 mm depth; (ii) for cavities of nominal 2-4 mm depth 24
Figure 16 – Locations of interest within wall assemblies in assessing relative performance 26
Figure 17 – Relatrive humidity (RH %) and tempeature (T°C) data averaged every 10 days over a 2 year period and representative of simulation conditions 28
Figure 18 - Comparison between the limits of applicability of the RHT index to that of the Mould index 30
Figure 19 - Comparison of simulation results over 4 storeys for Tofino, BC (MI = 3.4) 31
Figure 20 – Mould index for specified locations in wall assembly as a function of time over a 2 year simulation period for Tofino, BC 32
Figure 21 – Mould index for specified locations in wall assembly as a function of time over a 2 year simulation period for Vancouver, BC 33
Figure 22 – Mould index for specified locations in wall assembly as a function of time over a 2 year simulation period for St. John's, NL 33
Figure 23 – Locations in wall section of M_{IDX} values 34
Figure 24 – Mould index for 1 mm "Sliver" at exterior face of OSB panel of a 4th-storey wall for selected climate locations as a function of time over a 2 year simulation period 35
Figure 25– Mould index for the "Back" 10 mm portion of OSB panel of a 4th-storey wall for selected climate locations as a function of time over a 2 year simulation period Figure 26 - Mould index for the "Whole" 11 mm portion of OSB panel of a 4th-storey wall for selected climate locations as a function of time over a 2 year simulation period 35

Figure 27 - Mould index for interface between OSB panel and fibrous insulation of a 4th-storey wall for selected climate locations as a function of time over a 2 year simulation period..... 36
Figure 28 – Relative humidity (%) and temperature (°C) plot over a 2-year simulation period for a 1 mm "sliver" of OSB panel within a section of the reference wall of 4th-storey and subjected to Tofino climate 38
Figure A29 – Hourly WDR intensity for (a) St. John's, NL, (b) Vancouver and (c) Tofino, BC, over an "average" year 41
Figure A30 - Correlation for water permeation of a stucco- clad wall assembly..... 42
Figure A31- Correlation for water entry at deficiencies of through-wall ventilation duct 42
Figure A32 – Mould index of reference wall at 4th-storey for components having MR sensitivity class; Tofino 43
Figure A33 – Mould index values at each storey for components having MR sensitivity class; Tofino ... 43

List of Tables

Table 1 – 2010 National Building Code requirements for Capillary Breaks in Coastal areas (degree-days < 3400 and MI > 0.9, or degree days ≥ 3400 and MI > 1.0) 7
Table 2 – List of Wall Assemblies and Respective Characteristic Drainage Component 10
Table 3 – List of drainage components for which air flow was characterized 11
Table 4 – List of Canadian locations having MI > 1 12
Table 5 – Water entry correlation at deficiencies - Values of correlation coefficients for Eq. 4 21
Table 6 –Summary of Results Obtained for Depths of Venting and Drainage Cavities 22
Table 7 - Description of Mould Index (M) levels [18, 19, 20] 29
Table 8 - Mould growth sensitivity classes and some corresponding materials [20] 29
Table 9 - Mould growth sensitivity classes for different materials of wall assemblies 29
Table 10 –Mould index values used as performance attributes of wall assemblies 30
Table 11 – RHT index response of Reference Wall (OSB 1 mm thick sliver) 31
Table 12 – Mould index response of Reference Wall (OSB 1 mm thick sliver) 31
Table 13 – Values of RHT index for Selected climate locations 37

Acknowledgements

The report authors wish to extend their thanks to the Air Barrier Association of American (ABAA) for having managed and arranged support for this project and in particular, to Mr. Laverne Dalgleish for his highly proficient handling of all technical and non-technical issues that arose over the course of the project. As well, acknowledgment is made of project support, technical meeting participation and the many and very useful contributions made by the respective project partners, and that included:

Benjamin Obdyke Incorporated

Canadian Concrete Masonry Producers Association

Cosella-Dorken

DuPont Tyvek Weatherization Systems

HAL Industries Incorporated

Home Protection Office of British Columbia – HPO

Keene Building Products™

GreenGuard® Building Products (formerly Pactiv Building Products)

Roxul Incorporated

STO Corporation

TYPAR® Weather Protection System (Polymer Group Incorporated)

Our thanks are also extended to our colleagues within NRC-Construction for their technical support, advice, and feedback during the course of this project and who helped support the work described in this Task report including: M. Armstrong, S. Bundalo-Perc, S. M. Cornick, B. Di Lenardo, G. Ganapathy, W. Maref, T. Moore, P. Mukhopadhyaya, M. Nicholls, H. H. Saber, and M.C. Swinton and D. Van Reenen..

Summary

A benchmark assembly and a series of ten client wall assemblies were developed as part of the project "Performance Evaluation of Proprietary Drainage Components and Sheathing Membranes when Subjected to Climate Loads".

The purpose of this project was to assess the performance of wall drainage components and sheathing membranes (drainage system) in their ability to provide sufficient drainage and drying in Canadian climates with a moisture index (MI) greater than 0.9 and less than 3400 degree-days, or MI greater than 1.0 and degree days ≥ 3400 (primarily coastal areas). In these regions, the 2010 National Building Code of Canada (NBC) requires a capillary break behind all Part 9 claddings and conforming to the requirements given in § 9.27 (Cladding) of the NBC. Currently, acceptable solutions to the NBC capillary break requirement include:

(a) A drained and vented air space not less than 10 mm deep behind the cladding;

(b) An open drainage material behind the cladding, not less than 10 mm thick and with a cross-sectional area that is not less than 80% open;

(c) A cladding loosely fastened, with an open cross section (i.e. vinyl, aluminum siding);

(d) A masonry cavity wall or masonry veneer constructed according to § 9.20 (i.e. 25 mm vented air space).

In this project, the performance of proposed alternative solutions for the capillary break was compared through laboratory evaluation and modeling activities to the performance of a wall built to minimum NBC requirements. The proposed drainage system would be deemed an alternative solution to the capillary break requirement in the NBC for use with current code compliant Part 9 claddings provided it exhibited better or equal moisture performance as compared to a NBC-compliant benchmark wall assembly.

In This Report —

Results from hygrothermal simulation have been presented in which the response of the reference wall to climate conditions of Tofino (BC), Vancouver (BC), and St. John's (NL) have been described. The results, as provided by information on the mould index and RHT index within the assembly, permitted comparisons of the response of the reference wall to the different climates.

In addition, a thorough overview of the hygrothermal simulation model hygIRC-C has been provided and examples have been given on exercises undertaken to benchmark the model. As well, information has been provided regarding the inputs required to complete hygrothermal simulations and included:

- A summary description of the reference wall assembly and of Client wall assemblies in regards to their respective drainage component characteristics;
- Hygrothermal property characteristics
- Definition of climate loads for several Canadian locations, including information on the moisture index, annual driving rain index, rainfall, rainfall intensity, prevalent wind-driven rain direction, identification of "average" and "wet" years, and the selection of representative Canadian climate locations for simulation;
- Definition of moisture loads acting on components within the wall assembly: the amount of water entry to, and drainage from, wall assemblies and the amount of water retention in drainage systems; and
- Definition of performance attributes of wall components in terms of selected performance criteria including the mould index and RHT index.

Nomenclature

C_P	effective specific heat (J/(kg•K)
D_l	liquid diffusivity (m^2/s)
$\vec{g}$	vector of gravitational acceleration (m^2/s)
h_{fg}	latent heat of evaporation (J/kg)
h_{ls}	latent heat of fusion (J/kg)
k_l	liquid water permeability (s)
P	pressure (Pa)
R_v	water vapour gas constant (J/(kg•K))
$\vec{v}$	velocity vector (m/s)
T	temperature (K)
t	time (s)
w	moisture content (kg/m^3)

Greek Symbols

ε_0	porosity of porous material (-)
δ_P	vapour permeability (s)
ϕ	relative humidity ratio
ρ	density (kg/m^3)
μ	dynamic viscosity (Pa•s)
κ_a	air permeability (m^2)
ξ	specific moisture capacity (kg/m^3).
λ_{eff}	effective thermal conductivity (W/(m•K)

Subscripts

a	air
eff	effective
l	water liquid
o	solid matrix
v	water vapour
sat	saturation

Performance Evaluation of Proprietary Drainage Components and Sheathing Membranes when Subjected to Climate Loads –

Task 6 – Hygrothermal Performance of NBC-Compliant Reference Walls for Selected Canadian Locations

Authored by:

Hamed H. Saber and Michael A. Lacasse

A Report for the

AIR BARRIER ASSOCIATION OF AMERICA (ABAA)

1600 BOSTON-PROVIDENCE Highway
WAYPOLE, MA 02081
USA

ATT: Mr. Laverne Dalgleish

National Research Council Canada
Ottawa ON K1A 0R6 Canada

9 June, 2015

Performance Evaluation of Proprietary Drainage Components and Sheathing Membranes when Subjected to Climate Loads –

Task 6 – Hygrothermal Performance of NBC-Compliant Reference Walls for Selected Canadian Locations

Final Report Task 6

Hamed H. Saber and Michael A. Lacasse

1.0 Background and Introduction

The objective of this project was to assess the hygrothermal performance of wall assemblies incorporating drainage components. The ability of these wall assemblies to provide sufficient moisture dissipation through the process of drainage and drying of water from these components was evaluated. The wall assemblies evaluated were subjected to Canadian climates having a moisture index greater than 1.0. In these climates, the 2010 National Building Code of Canada (NBC) requires a capillary break behind all Part 9 claddings [1]. Currently, acceptable solutions to the NBC requirement for a capillary break include:

a) A drained and vented air space not less than 10 mm deep behind the cladding;
b) An open drainage material behind the cladding, not less than 10 mm thick and with a cross-sectional area that is not less than 80% open;
c) A cladding loosely fastened, with an open cross section (i.e. vinyl, aluminum siding);
d) A masonry cavity wall or masonry veneer constructed according to § 9.20 (i.e. 25 mm vented air space).

In this project, the hygrothermal performance of proposed alternative solutions for the capillary break was compared using laboratory testing and modeling activities to the performance of a wall (NBC code-compliant reference wall) built to minimum code requirements using the following performance criteria:

(a) RHT criterion, and;
(b) Mould index criterion.

If a proposed wall system incorporating a drainage component exhibits adequate performance as compared to the NBC code-compliant reference wall, it will be deemed an alternative solution to the 2010 NBC requirement for a capillary break and can be used with all code compliant Part 9 claddings [[1]].

The hygrothermal performance of wall assemblies incorporating drainage components was assessed on the basis of the results obtained from numerical simulation of a NBC code-compliant reference wall

[1] NBCC 2010 Part 9; Housing and Small Buildings; Cladding conforming to § 9.27

assembly when subjected to environmental loads for selected locations in Canada and conforming to interior boundary conditions as described in the ASHRAE Standard S-160 [[2]].

In this report, information is provided in four sections. The initial section (§2) consists of an overview of the hygrothermal simulation model, hygIRC-C. In the second section (§3), summary information, taken from the respective Task reports[3], is given on all necessary inputs to hygIRC-C, including brief descriptions of: hygrothermal properties; reference wall configuration; climatic loads acting on walls of a NBC Part 9 building from the wall exterior and those acting on the interior of the wall; water entry through cladding; water drainage and retention in wall assembly; size of drainage gaps of different assemblies incorporating drainage components, and; additional assumptions for completing hygrothermal simulations.

In the third section (§4), information is given on the manner in which performance attributes of specific components of the wall assembly were defined and on which basis the performance of the code compliant reference wall was assessed in relation to the client wall assemblies incorporating drainage components.

Finally, in the fourth section (§5), the detailed hygrothermal simulation results for the NBC code compliant reference wall are provided and the results are discussed.

The detailed hygrothermal simulation results for each of the partner wall assemblies (A to K inclusive) and in which the results are likewise discussed, are given in a companion report [3] (A1-000030.08).

2.0 Overview of Hygrothermal Simulation Model, hygIRC-C

The NRC's hygrothermal model, hygIRC-C, was used to predict the hygrothermal performance within wall assemblies having different drainage components. Results were analyzed on the basis of the risk of moisture-related effects when these walls were subjected to different climatic conditions as might occur across Canada. It is important to emphasize that the predictions by such a model for the airflow, temperature, and moisture (or relative humidity) distributions within a wall assembly, when subjected to a pressure differential (and resulting air leakage rate) across the assembly, are necessary to accurately determine the moisture response in different layers of the wall assembly.

The hygIRC-C model simultaneously solves the highly nonlinear and coupled two-dimensional and three-dimensional Heat, Air and Moisture (HAM) equations for both porous and non-porous media that define values of heat, air and moisture transfer across the various building component layers. The HAM equations were discretized using the Finite Element Method (FEM) as provided in the COMSOL Multi-physics software package that was used as a solver. The use of the FEM is important as it permits modeling complicated wall geometries with fewer discretizing errors.

2.1 Governing Equations

Three sets of governing equations define the transfer HAM for porous and non-porous media; each of these is described in turn.

[2] ASHRAE Standard S-160

[3] A list of all project reports for the different tasks (Task 1 to Task 7) is provided in Appendix 1

2.1.1 Air transport - Continuity and momentum

For an airspace (e.g. drainage cavity), the air velocity field, $\vec{v}_a$, and pressure field, P_a, are calculated by solving the continuity equation and momentum equation (compressible Navier-Stokes equation), each of which are respectively given as [4]:

$$\frac{\partial \rho_a}{\partial t} = -(\nabla \bullet (\boldsymbol{\rho_a \vec{v}_a})) \tag{1}$$

$$\boldsymbol{\rho_a} \frac{\partial \vec{v}_a}{\partial t} + \boldsymbol{\rho_a \vec{v}_a} \bullet \nabla \boldsymbol{\vec{v}_a} = -\nabla \boldsymbol{P} + \nabla \bullet \left(\boldsymbol{\mu_a} \left(\nabla \boldsymbol{\vec{v}_a} + (\nabla \boldsymbol{\vec{v}_a})^T \right) - \frac{2}{3} \boldsymbol{\mu_a} (\nabla \bullet \boldsymbol{\vec{v}_a}) \boldsymbol{I} \right) + \boldsymbol{\rho_a \vec{g}} \tag{2}$$

and where I is a 3 x 3 unit matrix.

For porous material layers, the continuity and momentum equations of air are respectively given as [4]:

Mass balance equation: $$\boldsymbol{\varepsilon_0} \frac{\partial \rho_a}{\partial t} = -(\nabla \bullet (\boldsymbol{\rho_a \vec{v}_a}) \tag{3}$$

Darcy's law: $$\boldsymbol{\vec{v}_a} = -\frac{\kappa_a}{\mu_a} (\nabla \boldsymbol{P_a} - \boldsymbol{\rho_a \vec{g}}) \tag{4}$$

where ε is the porosity (ratio of pore volume to total volume).

The supercritical air velocity $\vec{v}_a$ (Darcy velocity), is the volume rate of air flow through a unit cross sectional area of solid plus fluid, which is averaged over a small region of space (small in relation to the macroscopic dimensions of the flow system but large in respect to pore size). The air permeability κ_a is a scalar quantity for isotropic materials and a tensor quantity for anisotropic porous materials. Moreover, the air density, ρ_a, and pressure, P_a, are averaged over a region available to airflow that is large in respect to the pore size. An empirical modification of Darcy's law has been suggested by Brinkman as [4]:

$$\boldsymbol{0} = -\nabla \boldsymbol{P_a} - \frac{\boldsymbol{\mu_a}}{\boldsymbol{\kappa_a}} \boldsymbol{\vec{v}_a} + \boldsymbol{\mu_{a,eff}} \nabla^2 \boldsymbol{\vec{v}_a} + \boldsymbol{\rho_a \vec{g}} \tag{5}$$

In this modification, the term $\mu_{a,eff} \nabla^2 \vec{v}_a$ was introduced to account for the distortion of velocity profiles for which the momentum transport within the fluid due to share stresses is of importance. The parameter $\mu_{a,eff}$ is the effective viscosity that in theory takes into account the stresses borne by the fluid as it flows through the porous media. However, experimental measurement of $\mu_{a,eff}$ is not a trivial matter and based on the literature, its value is considered equal to the fluid viscosity, μ_s.

For flow in a porous media, a parameter called Darcy number, D_N, is introduced to define the type of flow regime within the porous media. D_N is a dimensionless parameter that is defined as the ratio of media permeability (κ_a) to the square of domain thickness, δ_{do} ($D_N = \kappa_a / {\delta_{do}}^2$). In the Darcy model, it is assumed that all of the stress in the flow field is carried by the porous media and the fluid is thus not subjected to any strain that arises due to viscous stresses. This assumption holds for flow through a porous media of low permeability where the flow velocity is small (i.e. Darcy flow). However, this assumption cannot be regarded to be physically realistic for porous media of high permeability where a

[4] Bird, R.B., Stewart, W.E., and Lightfoot, E.N. 1960. Transport Phenomena, John Wiley & Sons, Inc., pp. 149-150

part of the viscous stress is borne by the fluid itself, and which is in the Brinkman equation accounted for by the term $\mu_{a,eff}\nabla^2\vec{v}_a$ (see Eq. (5)). As such, the Brinkman equation should be used to characterise flow through highly permeable porous media given that this equation accounts for the transition from Darcy to viscous flow. This topic has been studied by many investigators [5, 6, 7, 8].

The present model was used to conduct a simple numerical test in order to identify the different flow regimes in porous media. In this test, a porous layer (140 mm thick) was sealed at the top and bottom and subjected to a pressure difference across it (Figure 1 insert). To cover a wide range of values for D_N, the numerical test was likewise conducted using a broad range of values for air permeability.

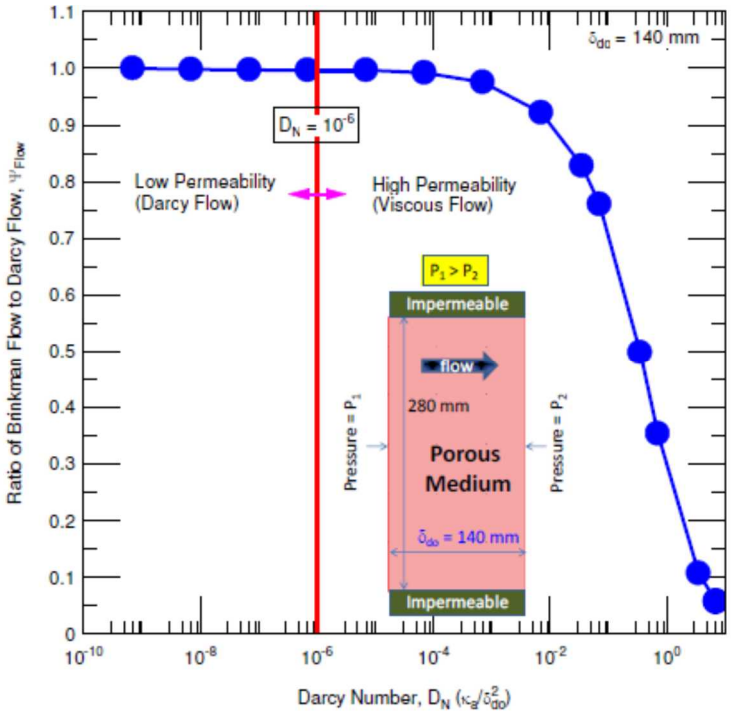

Figure 1 – Dependence of airflow ratio, Ψ_{Flow}, on Darcy number, D_N [9]

Figure 1 shows the dependence of the airflow ratio, Ψ_{Flow} on the Darcy number, D_N. The value of Ψ_{Flow} is defined as the ratio of net airflow rate, obtained from solving the Brinkman equation (Eq. (5)), to that obtained from solving Darcy's law (Eq. (4)). As shown in this figure, the airflow rate obtained from solving Darcy's law and the Brinkman equation are equal (i.e. Ψ_{Flow} = 1.0) for flow through a porous media of low permeability (i.e. $D_N = 10^{-6}$, Darcy flow regime), where the effect of the viscous stress term in the Brinkman equation is insignificant. However, for flow through a highly permeable porous media

[5] D.A. Nield & A. Bejan (1992), Convection in Porous Media, Springer-Verlag, New York,

[6] M. Parvazinia, V. Nassehi, R. Wakeman, M.H.R Ghoreishy, (2006), Finite element modeling of flow through a porous medium between two parallel plates using the Brinkman equation, Transport in Porous Media, 6; pp.71-90.

[7] Satya Sai, B.V.K.; Sitaramu, K. N., and; Aswathanarayana, P. A. (1997), Finite element analysis of heat transfer by natural convection in porous media in vertical enclosures, Int. J. Numerical Methods Heat Fluid Flow, 7; pp. 367-400.

[8] M. Kaviany, (1985), Laminar flow through a porous channel bounded by isothermal parallel plates, Int. J. Heat Mass Trans., 28 pp. 851–858.

[9] Saber, H. H.; Maref, W.; Swinton, M. C.; St-Onge, C. (2011), Thermal analysis of above-grade wall assembly with low emissivity materials and furred-airspace; Journal of Building and Environment, 46 (7), p. 1403-1414

with (i.e. $D_N = 10^{-6}$, viscous flow regime), Darcy's law over predicts the airflow rate (i.e. $\Psi_{Flow} < 1.0$). As is shown in Figure 1, and in accordance with that described by Parvazinia et al. [6], the flow can be described by Darcy's law $D_N \leq 10^{-6}$, whereas the Brinkman equation should be used to characterise the flow when $D_N > 10^{-6}$. An accurate prediction of the airflow through porous media is essential to correctly account for moisture transport and energy transfer by convection through these materials.

When Eqs. (3) and (4) are combined, the equation of motion of air through a porous medium is rewritten as:

$$\boldsymbol{\varepsilon_0 \frac{\partial \rho_a}{\partial t} = \nabla\bullet\left(\rho_a \frac{\kappa_a}{\mu_a}(\nabla P_a - \rho_a \vec{g})\right)} \quad (6)$$

2.1.2 Heat Transfer

The energy balance equation in a porous media for the fluid (air) and solid phases is obtained from the local volume averaging in terms of fluid and solid temperatures. An averaging volume should be sufficiently small to permit distinguishing the overall structure of flow but large enough to contain both fluid and solid phases throughout the structure at all times. Such a volume is termed a Representative Elementary Volume (REV) as is illustrated in Figure 2. In many practical applications, the temperature difference between the solid and fluid phases within a REV is much smaller than the overall temperature variation of the material [11, 12]. This condition is met if the REV is much smaller as compared to the overall length scale [13]. Under this condition, the temperatures of the fluid and solid phases could be assumed equal to the local thermodynamic equilibrium temperature, T.

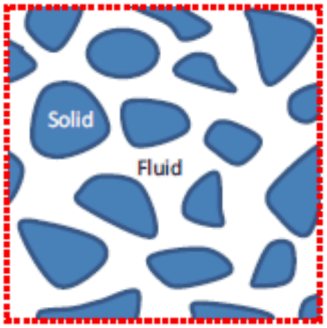

Figure 2– Schematic illustrating a Representative Elementary Volume (REV) in porous media [10]

Based on this assumption, the air transport mass balance equation (Eq. 3) and the energy equation for the fluid phase and the energy equation of the solid phase can be combined to one energy equation as:

$$\frac{\delta}{\delta t}\left(\left(\varepsilon\rho_a C_{P_a} + (1-\varepsilon)\rho_S C_{P_s}\right)T\right) + \nabla\bullet\left(\rho_a C_{p_a}\vec{v}_a T\right) = \nabla\bullet\left((\varepsilon\lambda_a + (1-\varepsilon)\lambda_s)\nabla T\right) + q'''_{srce/sink} \quad (7)$$

For porous media, the density is given as, $\rho_0 = (1-\varepsilon)\rho_s$, the effective thermal conductivity $\lambda_{eff} = \varepsilon\lambda_a + (1-\varepsilon)\lambda_s$, and the effective specific heat capacity as $C_{P_{eff}} = C_{P_s} + \varepsilon C_{P_a}(\rho_a/\rho_0)$, Equation (7) can now be re-written as:

$$\underbrace{\boldsymbol{\rho_0 C_{p_{eff}} \frac{\partial T}{\partial t}}}_{\text{Storage}} + \underbrace{\left(C_{p_a}\rho_a\overrightarrow{v_a}\bullet\nabla T\right)}_{\text{Heat convection}} = \underbrace{\nabla\bullet\left(\lambda_{eff}\nabla T\right)}_{\text{Heat conduction}} + \underbrace{h_{fg}(T)(\nabla\bullet\delta_P\nabla P_v - \nabla\bullet\rho_a\overrightarrow{v_a})}_{\text{Heat source / sink due to evaporation / condensation}} + \underbrace{h_{ls}(T)\frac{\partial w_{ice}}{\partial t}}_{\text{Heat source / sink due to freezing / thawing}} \quad (8)$$

[10] Saber, H. H.; Maref, W.; Elmahdy, A. H.; Swinton, M. C.; Glazer, R. (2012), 3D heat and air transport model for predicting the thermal resistance of insulated wall assemblies, International Journal of Building Performance Simulation, 5(2): p. 75-91

[11] Vafai, K., and Tien, C.L. 1981. Boundary and inertia effects

[12] Pakdee, W., & Rattanadecho, P. 2006. Unsteady effects of natural convective heat transfer through porous media in cavity due to top surface partial convection. Applied Thermal Engineering, 26, pp. 2316-1326.

[13] Sozer, E., and Shyy, W. 2008. Multi-scale thermo-fluid transport in porous media. Int. J. of Numerical Methods for Heat & Fluid Flow, 19 (7), pp. 883-899.

2.1.3 Moisture Transfer

The moisture transfer is given by:

$$\frac{\partial w}{\partial t} = -\nabla \bullet \begin{bmatrix} -\left(\boldsymbol{\delta_P} + \frac{\boldsymbol{D_l \xi}}{\boldsymbol{P_{v,sat}}}\right) \nabla \boldsymbol{P_v} + \boldsymbol{k_l \rho_l \vec{g}} + \boldsymbol{\rho_v \overrightarrow{v_a}} \\ -\left(\frac{\boldsymbol{\phi D_l \xi}}{\boldsymbol{T}}\left(\ln(\boldsymbol{\phi}) - \frac{\boldsymbol{h_{fg}}}{\boldsymbol{R_v T}}\right) - \boldsymbol{\delta_P}\frac{\boldsymbol{P_v}}{\boldsymbol{T}}\right) \nabla \mathbf{T} \end{bmatrix} \quad (9)$$

Where $\boldsymbol{\delta_P}$ is the vapour permeability (s); $\boldsymbol{D_l}$ the liquid diffusivity (m^2/s); $\boldsymbol{\xi}$, the specific moisture capacity (kg/m^3); $\boldsymbol{k_l}$ the liquid water permeability (s); $\boldsymbol{P_{v,sat}}$ the saturation vapour pressure (Pa); $\boldsymbol{h_{fg}}$, the latent heat of evaporation (J/kg); $\boldsymbol{R_v}$, the water vapour gas constant (J/(kg•K), $\boldsymbol{\rho}$, density (kg/m3); and $\boldsymbol{T}$, temperature (K).

2.2 Hygrothermal Simulation Model Validation

The hygIRC-C model has been extensively validated in a number of other projects in which the thermal and hygrothermal performance of different systems and components of the building envelope (e.g. roofing, wall and fenestration systems) were evaluated; a review of the different projects in which the model was benchmarked is given in the Task 3 Report [3] (A1-000030.04).

Additionally, in this project two specific benchmarking exercises were conducted to verify whether proper assumptions had been made in regards to the mathematical and numerical representation of physical phenomena within the hygIRC-C model and in capturing the hygrothermal response of components within wall assemblies; these included benchmarking the:

- Moisture dissipation from a nominally saturated stucco plate conforming to NBC compliant stucco construction details when subjected to ambient laboratory conditions; the results from this work, included in the Task 3 Report, indicated that the model correctly estimated the degree and rate of moisture dissipation over time with a variation in values of moisture content not exceeding ± 5% from that predicted by the simulation model.
- Air flow through clear cavities and cavities incorporating highly porous media used as drainage components in wall assemblies; the results from these tests are provided in the Task 4 Report (A1-000030.05) [3].
    - Clear Cavities — A comparison of test results to those derived from simulation showed that the majority of air velocity measurements were within the margin of uncertainty associated with the results derived from simulation for air velocity profiles obtained of cavities having depths of 10, 20 and 25 mm.
    - Non-homogenous highly porous media (drainage components) — The air permeability, κ_a, was shown to be pressure dependent and deviations from the test values were minimized provided the value for κ_a was selected in relation to the pressure difference acting along the length of the cavity incorporating the drainage media. As such, values for the effective permeability coefficient, κ_{eff} and corresponding values for the permeability factor, F, were provided in relation to the pressure difference across the drainage components.

3.0 Description of Wall Assemblies & Hygrothermal Property Characterization

3.1. Description of Wall Assemblies (Task 1)

The purpose of this project was to assess the performance of wall drainage components and sheathing membranes in their ability to provide sufficient drainage and drying in Canadian climates with a moisture index (MI) greater than 0.9 and less than 3400 degree-days, or MI greater than 1.0 and degree days ≥ 3400 (primarily coastal areas), as described in Table 1. In these regions, the 2010 NBC requires a capillary break behind all Part 9 claddings.

Table 1 – 2010 National Building Code requirements for Capillary Breaks in Coastal areas (degree-days < 3400 and MI > 0.9, or degree days ≥ 3400 and MI > 1.0)

Coastal areas (degree-days < 3400 and MI > 0.9, or degree days ≥ 3400 and MI > 1.0)			
Sheathing	**Number of Sheathing Membranes**	**Capillary Break**	**Part 9 Claddings**
NO Sheathing	2	10-mm vented air space (80% open) or drainage material (80% open) or Alternative Solution	Lumber siding Wood shingles & shakes Fiber cement shingles and sheets(n/a) Plywood OSB and waferboard Hardboard Metal siding (horizontal or vertical) Vinyl siding (horizontal or vertical) Stucco
OSB/Plywood (Installed but not required)	1		
OSB/Plywood (Required and installed)	2		
OSB/Plywood	1 or, 2	25-mm vented air space	Masonry veneer

The approach used in this evaluation had a benchmark wall assembly against which the various client wall assemblies incorporating wall drainage components and sheathing membranes were compared in respect to their hygrothermal performance. A brief description of the benchmark wall assembly and client assemblies follows.

3.1.1 Reference Wall Assembly

The reference wall assembly was developed based on minimum code requirements. Stucco cladding was chosen from among the Part 9 claddings (listed in Table 1), as the "worst case scenario" for water penetration. This selection was based on previous work at NRC on the moisture management for exterior wall systems [14], in which it was demonstrated that stucco resulted in the highest moisture load behind the primary line of protection, due to its absorptive properties and rain penetration at cracks.

[14] NRC, Final Report from Task 8 of MEWS Project (T8-03) - Hygrothermal Response of Exterior Wall Systems to Climate Loading: Methodology and Interpretation of Results for Stucco, EIFS, Masonry and Siding-Clad Wood-Frame Walls; Research Report, NRC Institute for Research in Construction, 2002-11-01

Two alternative code compliant solutions for stucco installation were considered (see Figure 3):

- A solution predominantly practiced on the West Coast, with paper-backed welded wire mesh lath, and a 10 mm clear cavity;
- A solution predominantly practiced on the East Coast, with expanded metal lath (no paper backing) installed on 19 mm strapping.

The East Coast solution was selected for the reference wall assembly, and deemed to be the "worst case scenario" due to the ability for stucco to pass through the metal lath and into the drainage cavity. Unlike the West Coast solution, this East Coast wall has no layer of building paper behind the lath to reduce the possibility of stucco compromising the required clear 10 mm capillary break between the stucco cladding and back-up wall.

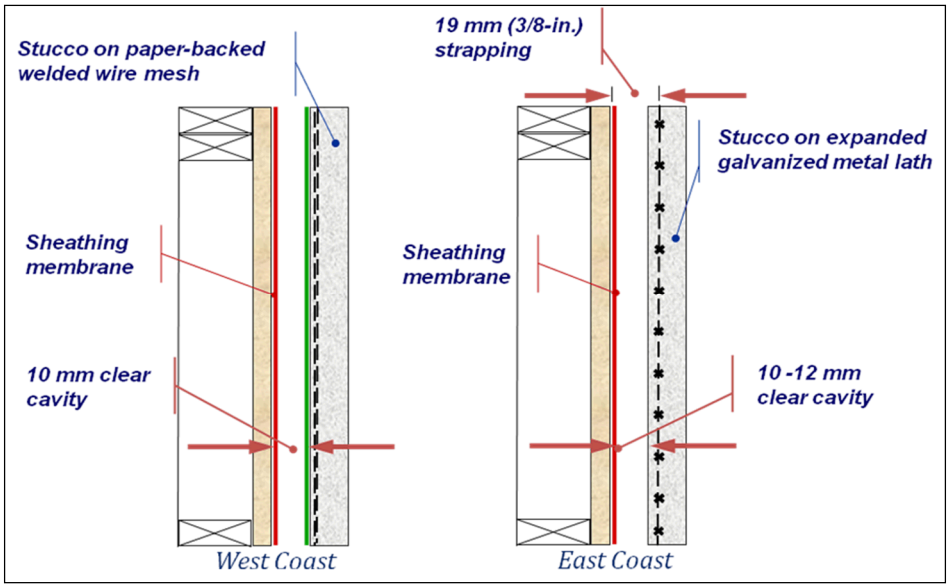

Figure 3 – West and East coast solutions for stucco installation with capillary break

The NBC additionally requires the wall to be vented and flashed at the bottom of the wall every 3.5 storeys. Whereas the constructed wall assemblies for lab evaluation were 1.83 m (6 ft.) in height, subsequent modeling activities took into account the performance of the full 3.5 storey assembly, including the influence of associated rain and wind loads on hygrothermal performance.

A duct penetration detail is included in the assembly drawings. Experimental work in this project examines and quantifies the potential for water to enter at a deficiency in the sealant around a duct penetration. This information is then used to determine realistic amounts of water to be introduced in the drainage and drying evaluation of the different assemblies.

A cross sectional view of the selected NBC code-compliant reference wall assembly is presented in Figure 4. Full details of the reference wall assembly and components are provided in the Task 1 report [3].

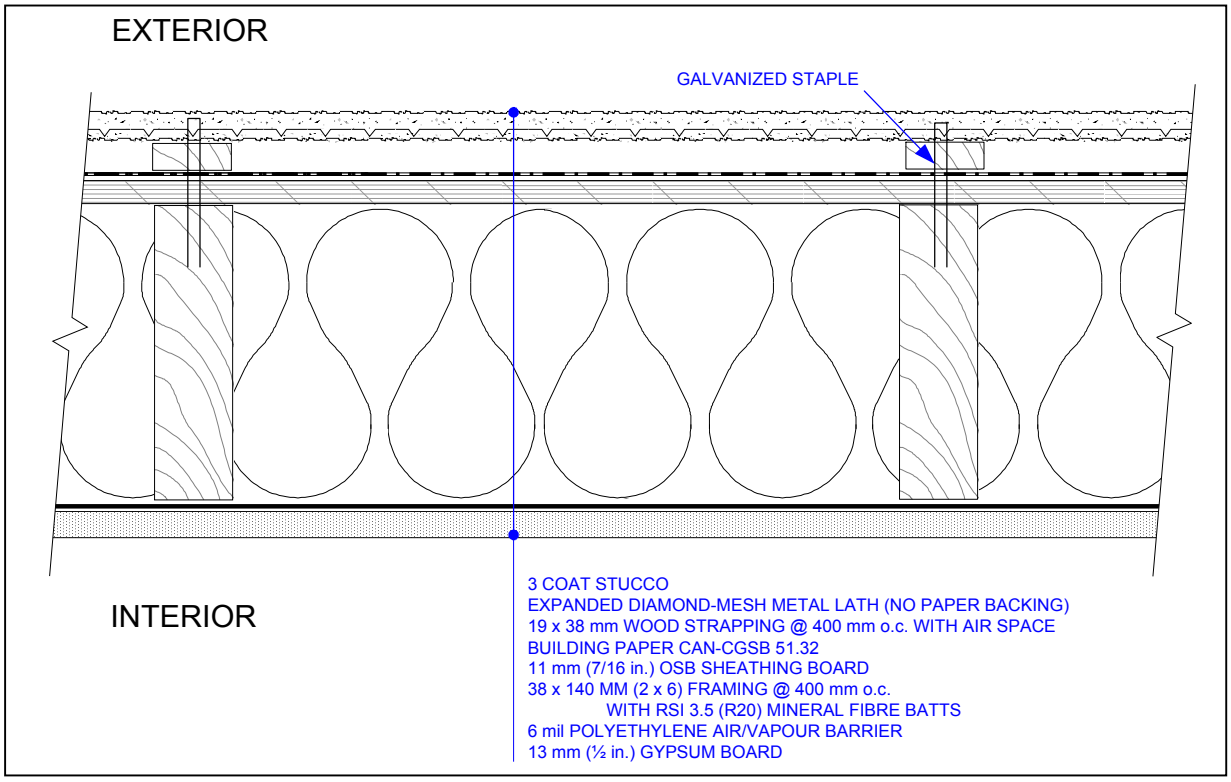

Figure 4 – NBC code-compliant reference wall - Horizontal cross section

3.1.2 Client Wall Assemblies

Client assembly designs were based on consultations between the individual clients and NRC-Construction; a list of client wall assemblies and their respective characteristic drainage component is provided in Table 2. In the companion report (A1-000030.08) [3], which includes the results of numerical simulation for the client wall assemblies, a summary is given of the elements of the respective client wall assemblies.

Of note is that all client walls featured the same stucco cladding as the benchmark wall. This cladding was chosen as a "worst case scenario". Thus, if the drainage element of the assembly demonstrated the ability to manage the water loads introduced by the stucco cladding, it was deemed an acceptable drainage solution suitable for use with all code compliant claddings, as given in Table 1. In the Task 1 report, cross sectional diagrams are provided for each wall assembly together with a table describing the elements that differ from the NBC code-compliant reference wall assembly.

Table 2 – List of Wall Assemblies and Respective Characteristic Drainage Component

Designations	Description of Drainage Component	Description of component tested for hygrothermal properties
Code-compliant Reference wall	Air space created by 19 mm plywood strapping; on NBC Code-compliant building paper*	NBC Code-compliant stucco
Client A Wall	Code compliant building paper* / cap fasteners provide 2 mm gap / SBPO** sheathing membrane	Drainable SBPO sheathing membrane
Client B Wall	10 mm air space / Water repellent insulation board (76 mm) / liquid applied membrane	Water repellent insulation board
Client C Wall	Code compliant building paper* / Nylon mesh (10 mm; open matrix) / PP† nonwoven sheathing membrane	Nylon mesh (10 mm; open matrix) bonded to PP nonwoven sheathing membrane
Client D Wall	Code compliant building paper* / Cap fasteners provide 2 mm gap / Cross woven, micro-perforated polyolefin sheathing membrane with polyolefin coating	Cross woven, micro-perforated polyolefin sheathing membrane with polyolefin coating
Client E Wall	PP† fabric (stucco screen) / Dimpled HDPE‡ (11 mm) membrane / Code compliant building paper*	PP† fabric bonded to dimpled HDPE‡ membrane
Client F Wall	Wall having 25 mm air space	Nil (25 mm air space)
Client G Wall	Non-woven PP† fabric (stucco screen) / PP† mat (10 mm; 3-dimensional extruded PP mono-filament mesh) / Code compliant building paper*	Non-woven PP† fabric (stucco screen) / PP† mat (10 mm; 3-dimensional extruded PP mono-filament mesh)
Client H Wall	Porous PS†† insulation board (52 mm) / liquid applied membrane	Porous PS†† insulation board (52 mm)
Client I Wall	2 ply, corrugated asphalt impregnated paper*; Grade D!! (4.2 mm) / Code compliant building paper*	2 ply, corrugated asphalt impregnated paper* - Grade D!!
Client J Wall	Building paper*; Grade D!!; 60 Minute / Air space created by 9.5 mm plywood strapping / 2 layers of Code compliant building paper*	Three coat stucco with paper backed welded-wire mesh lath
Client K Wall	Building paper*, Grade D!!; 60 Minute / Air space created by 9.5 mm plywood strapping / 2 layers of Code compliant building paper*	Three coat stucco with paper backed welded wire metal lath

* CAN-CGSB 51.32; ** SBPO – Spun bonded polyolefin; † PP – poly propylene; ‡ HDPE – high-density polyethylene; †† PS – polystyrene; !! Grade D – Building paper conforming to US Federal specification UU-B-790a, Type 1 (barrier paper), Grade D (water-vapor permeable), Style 2 (uncreped, not reinforced, saturated).

3.2 Task 2 (Hygrothermal Property Characterization)

To carry out hygrothermal performance assessments of wall assemblies using the numerical simulation tool hygIRC-C, the hygrothermal properties of all materials used for the construction of the different wall assemblies were required as input to the model. Given that a number of the hygrothermal properties of materials of the wall assemblies were available in NRC's material properties database, only the hygrothermal properties and air flow characteristics of materials that were not available were measured as part of this study, as given in Table 2; the designated client wall in which the materials were used is also identified in this table.

In addition, to permit quantifying the drying potential of various drainage layers, the air flow characteristics of the selected drainage components described were examined; a list of drainage layers for which air flow was characterized is given in Table 3.

A detailed account of the tests methods used to characterise and the resulting values obtained from tests of the hygrothermal properties of wall assembly components and air flow characteristics of the drainage components are given in the Task 2 report (A1-000030.02) [3].

Table 3 – List of drainage components for which air flow was characterized

Description of ventilation layer	Wall Designation
Empty ventilation cavity (7mm)	Reference
Nylon mesh (7 mm; open matrix)	Client C
Nylon mesh (7 mm; open matrix) bonded to PP nonwoven sheathing membrane	Client C
Non-woven PP† fabric (stucco screen) bonded to 10 mm; 3-dimensional extruded PP† mono-filament mesh	Client G
PP† fabric bonded to dimpled HDPE‡ membrane	Client E
2 ply, corrugated asphalt impregnated paper*; Grade D**	Client I

†PP – polypropylene; ‡ HDPE – High-density polyethylene; * Sheathing membrane (breather type) conforming to specification CAN-CGSB 51.32 ** Grade D – Building paper conforming to US Federal specification UU-B-790a, Type 1 (barrier paper), Grade D (water-vapor permeable), Style 2 (uncreped, not reinforced, saturated).

3.3 Defining Climate Loads on Wall Assembly & Drainage Systems (Task 5)

There were two primary objectives for this Task that included determining the:

- Climate loads to be used for testing wall assemblies;
- Weather data for the hygrothermal simulation task of the project (Task 6).

Each is described in turn.

3.3.1 Climate loads for testing wall configurations

Determining the environment loads to be used for testing wall configurations consisted of establishing the appropriate wind-driven rain loads, expressed in terms of a combination of water spray rate and driving-rain wind pressure, for key locations in Canada. The task involved collecting the appropriate weather data from vetted sources, identifying the locations of interest for the project, producing datasets for each location, and performing statistical analysis on each dataset to determine the exterior loading for each location.

All the Canadian locations having a MI value of one or greater and with a least 8 years of hourly climate data were identified as shown in Figure 5. Eleven MI bands between MI ≥ 1 and MI ≥ 2 were defined and representative locations within each band were identified. Two criteria were used to select representative locations within a band: (i) greatest MI value within the band, and; (ii) highest annual Driving Rain Index. If the two highest values did not correspond to a single location then both locations were selected. The method is summarized below.

The proposed list of Canadian locations is given in Table 4. Although not meeting the criteria, Vancouver BC was also included because of the history of moisture related problems in Vancouver.

Table 4 – List of Canadian locations having MI > 1

Station	MI	Rainfall, mm	Wind speed, km/h	aDRI, m^2/s
Tofino A. BC	3.36	3257	10.6	9.6
Port Hardy A. BC	1.92	1808	11.4	5.7
Abbotsford A. BC	1.59	1508	8.8	3.7
Halifax Int'l. NS	1.49	1239	16.8	5.8
Vancouver Int'l. BC	1.44	1155	11.8	3.8
St. John's A. NL	1.41	1191	23.3	7.7
Sydney A. NS	1.36	1213	18.6	6.3
Saint John A. NB	1.27	1148	16.1	5.1
Stephenville A. NL	1.19	985	19.2	5.3
Bonavista NL	1.11	816	31.7	7.2
Terrace A. BC	1.08	970	13.4	3.6
Summerside A. PE	1.03	806	20	4.5

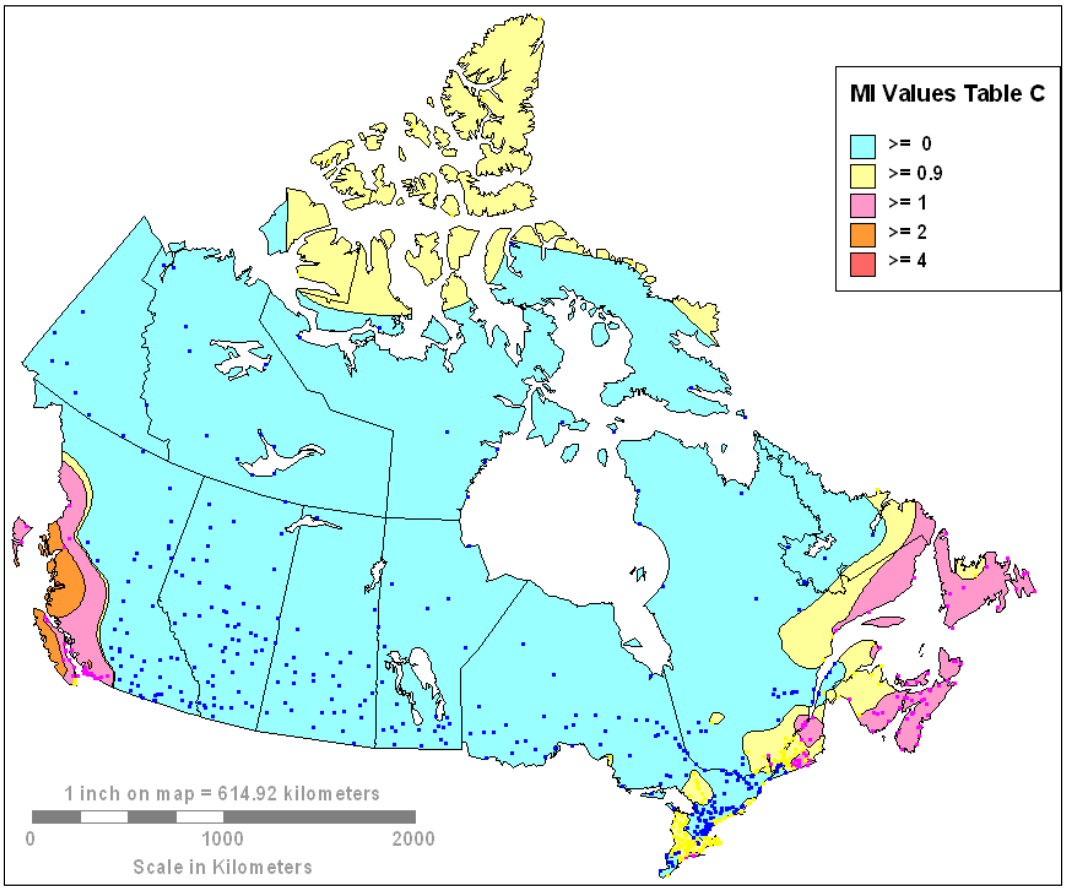

Figure 5 – Distribution of locations having MI > 1

A database of hourly data for each Canadian location was produced. Statistical analysis of the datasets produced the following values for Wind-Driven Rain (WDR) and Driving-Rain Wind Pressure (DRWP):

- Mean
- Median
- Standard deviation
- Maximum DRWP and WDR observed and coincident WDR or DRWP
- 98-percentile value of DRWP and WDR and coincident mean WDR or DRWP
- 1 in 50-year return period value

For all the Canadian locations analysed, a spray of 1 L/min-m^2 (or 60 L/hr-m^2) was sufficient to cover all locations and conditions for WDR. Similarly, a differential pressure of 500 Pa was sufficient to cover all values of DRWP. Note that the values of these thresholds are limited to a height of 10 m or less and time averages of 1-hour.

The maximum and 50-year return period values for wind-driven rain intensity (WDR) and driving-rain wind pressure (DRWP) for Canadian locations are provided in Figure 6 and Figure 7, respectively.

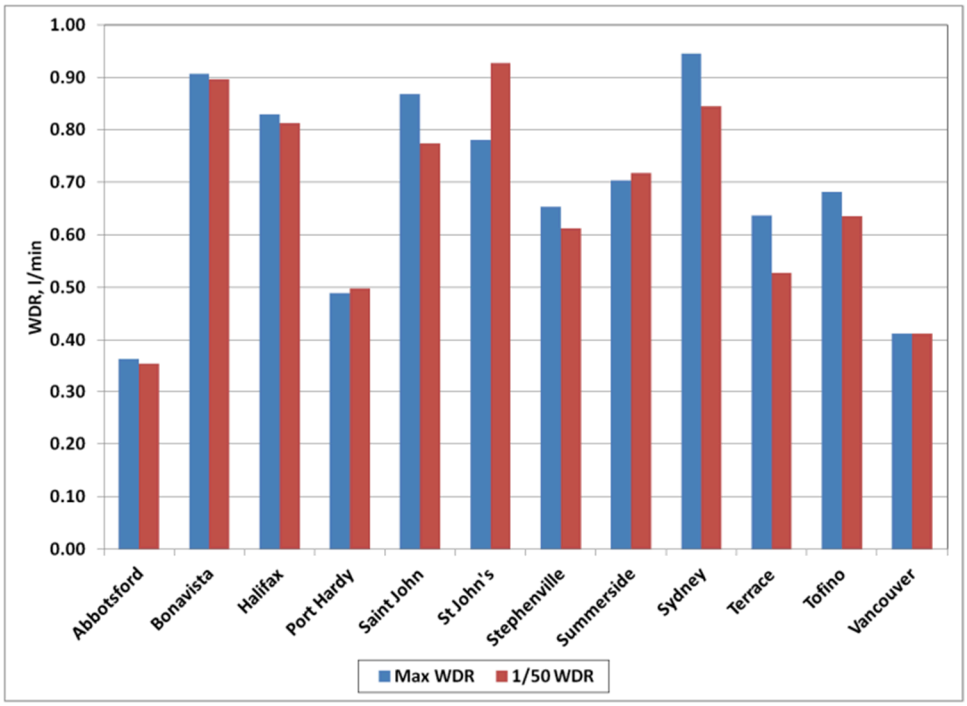

Figure 6 – Maximum and 50-year return WDR in L/h (a) and L/min (b) for Canadian locations

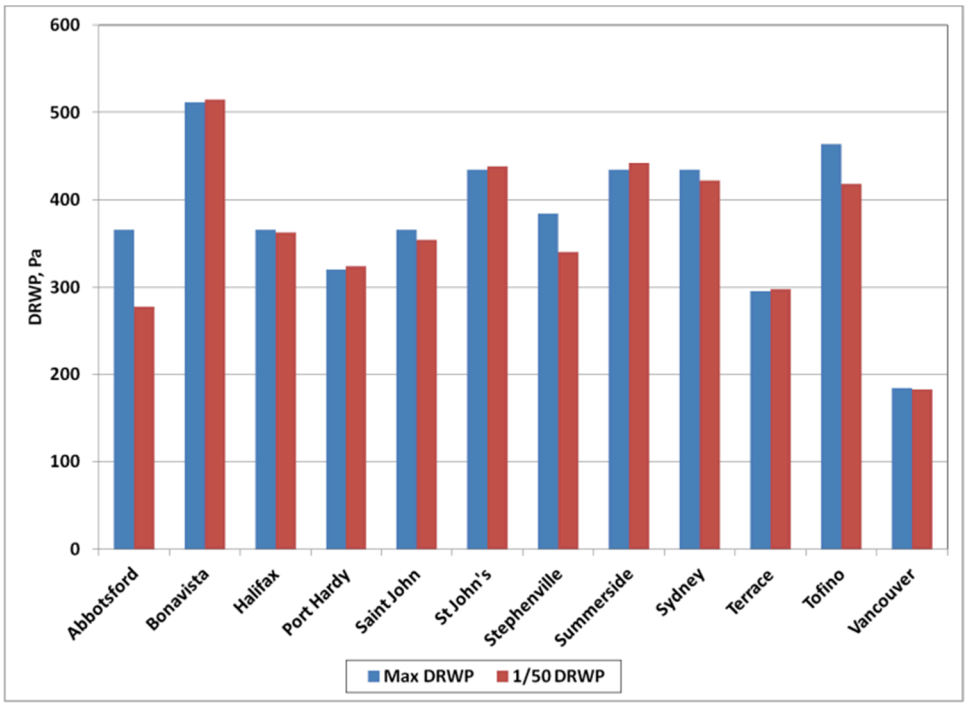

Figure 7 – Maximum and 50-year return DRWP in Pa for Canadian locations

3.3.2 Weather data for hygrothermal simulation

The second objective of the work was to determine and provide the Moisture Design Reference Years (MDRYs) data for the hygrothermal simulation task of the project. Appropriate climate data for this task was provided for the locations identified in Table 4.

After reviewing several published methods for selecting weather years for hygrothermal simulation, a small comparison study was undertaken. It was concluded that the MI MEWS method was appropriate to use for this project. Rankings were produced for all the years in the climate record for each location selected. Three years, *wet* (maximum), *average* (median), and *dry* (minimum), were generated and converted to an acceptable format for hygrothermal analysis.

Of these sets, hygrothermal simulations for selected locations were undertaken for an *average* (median), followed by a *wet* (maximum) year. The locations of interest were: St. John's (East coast climate – wet and cool, MI = 1.41), Vancouver (West coast climate – wet and mild, MI = 1.44) and Tofino (Extreme coastal climate having MI = 3.4).

The directional average yearly WDR intensity for St. John's (NL), Vancouver, and Tofino (BC), are provided in Figure 8. In Figure 8, the prevailing direction of maximum WDR intensity has been identified for each of these three locations. The prevailing direction of WDR for the West coast locations is easterly, whereas for the East coast location of St. John's, the WDR is primarily from the southerly direction.

The intensity of the maximum average WDR in St. John's is ca. 0.14 mm/h; in comparison, Vancouver has a similar intensity of ca. 0.10 mm/h, whereas Tofino has a threefold greater maximum average WDR of ca. 0.36 mm/h.

Some additional information regarding climate loads for these three locations is provided in Figure 9. The average WDR intensity, the total WDR, the number of rain events, and the average outdoor RH (%) are provided for a 2 year period for which the first year was an average year and the second a "wet" year. The data in these figures highlights the differences between the climate loads used in simulations for these three locations.

It is evident that Tofino has the most severe climate with respect to WDR loads, as the cumulative total WDR (6238 kg/m^{2}hr) is ca. 2.5 to 3.5 times more severe than that of St. John's (2428 kg/m^{2}hr) and Vancouver (1794 kg/m^{2}hr), respectively. This is also reflected by the number of rain events, with Tofino (2833) having twice that of St. John's (1411), but a similar quantity to Vancouver (2362).

The average values for outdoor relative humidity over a 2-year period (average year followed by a wet year) are all in the same order of magnitude for the three locations; however, the highest value is found in Tofino (89% RH), the next highest is St. John's (84% RH), followed by Vancouver (82% RH). For any of these coastal locations, the ability of moisture to dissipate from wetted wall assemblies is limited by the capacity of the ambient air to absorb moisture, which is more difficult in climates having higher average relative humidities.

St. John's, NL
AVG Year: 1959
WET Year: 1968

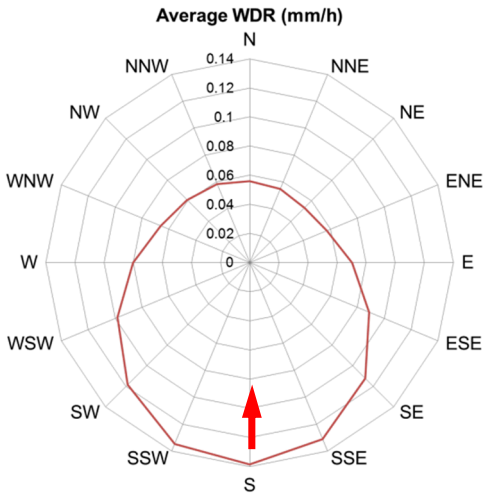

Vancouver, BC
AVG Year: 1969
WET Year: 1980

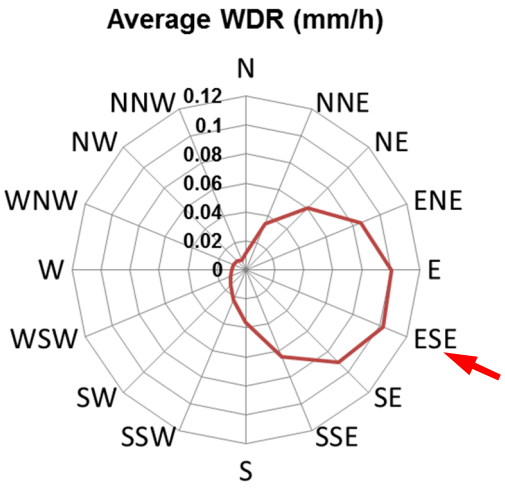

Tofino, BC
AVG Year: 1965
WET Year: 1961

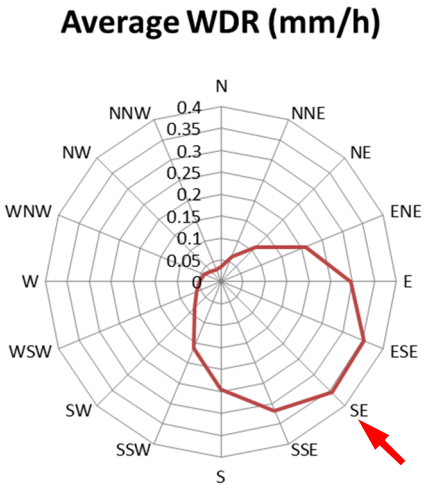

Figure 8 – Directional average yearly WDR intensity for (a) St. John's, NL, (b) Vancouver and (c) Tofino, BC, showing prevailing direction of maximum WDR intensity

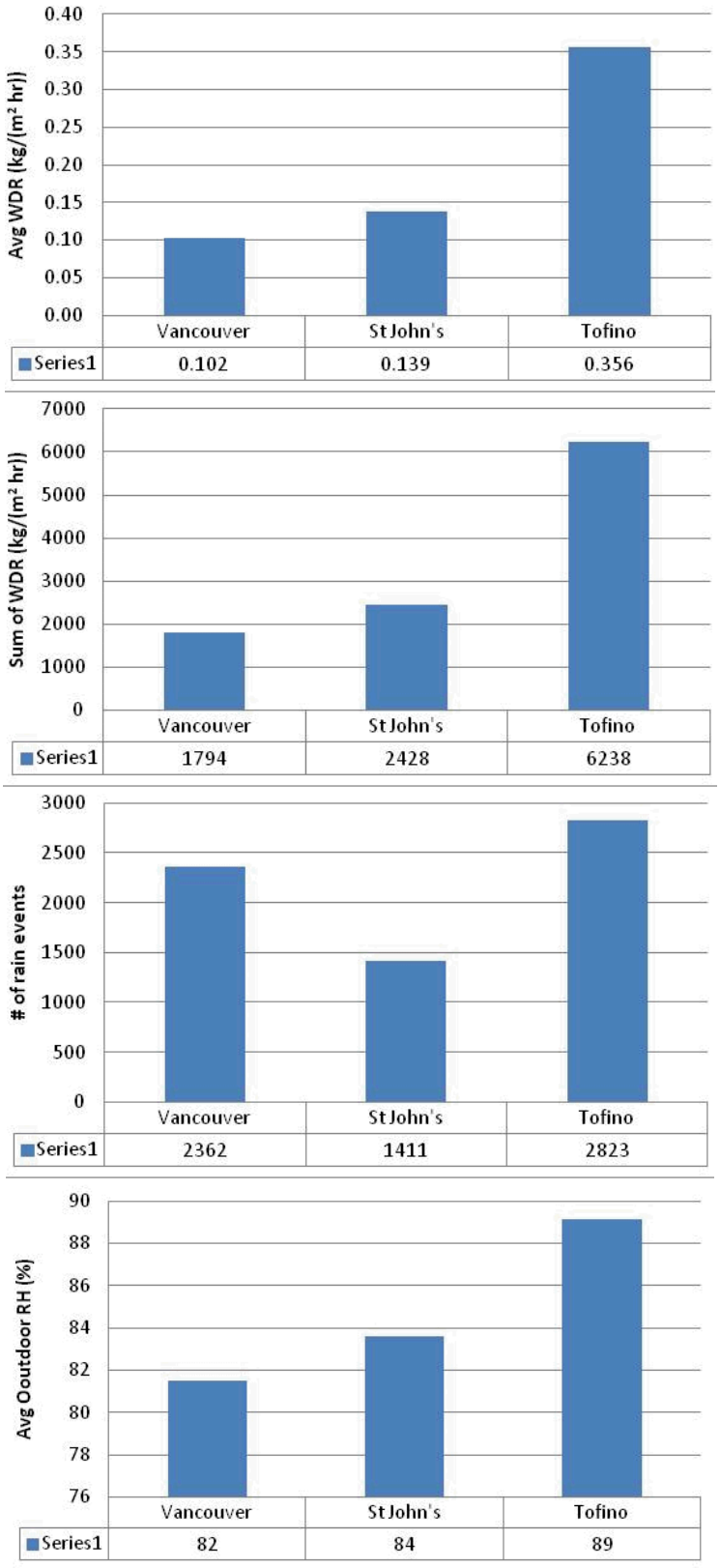

Figure 9– Average WDR intensity; Cumulative Total WDR; Number of rain events; Average outdoor RH (%) over 2 years (AVG & WET year) for Vancouver, St. John's and Tofino

3.4 Response of Wall Assemblies & Drainage Systems to Climate Loads (Task 5)

3.4.1. From climate loads to wind-driven rain loads acting on wall assembly and cladding

The scenario considered in estimating the hygrothermal response of wall assemblies and drainage systems to climate loads is provided in Figure 10, which includes an illustration of the wind-driven rain (WDR) and driving-rain wind pressure (DRWP) loads acting on the walls.

The DRWP acts along the full height of the wall assembly and changes in relation to the height above ground level according to the relationship:

$$\boldsymbol{v_z = v_g \left(\frac{z}{z_g}\right)^{\frac{1}{\alpha}}, 0 < z < z_g} \quad (10)$$

Where:

v_z = speed of the wind during rain event at height z
v_g = gradient wind speed at gradient height z_g (i.e. 10 m)
α = exponential coefficient (value from 0.27 (suburban terrain) to 0.60)

The amount of WDR that impinges on the exterior cladding of the wall assembly is a function of the horizontal rainfall intensity, and the DRWP, and may be estimated as:

The rate at which driving rain is incident on an unobstructed imaginary wall surface can be calculated from the rainfall rate and wind speed using empirical relationships between rainfall rate and drop size distribution [15] and drop size and terminal velocity [16], as expressed in Equation (11):

$$\text{WDR} = \frac{2}{9} v R_h^{\frac{8}{9}} \cos(\Theta - 90) \quad (11)$$

Where:

$\boldsymbol{v}$ = wind speed against the wall in m/s;
R_h = horizontal rainfall intensity in mm/hr; and
$\boldsymbol{\Theta}$ = wind direction.

As such, and given the increase in wind speed with height, the WDR intensity varies as the height of the building as illustrated in Figure 10.

3.4.2 Water entry behind cladding due to permeation of cladding and deficiencies

Water entry to the drainage system behind the cladding may come about due to water permeation through the cladding itself, or through imperfections at the periphery of cladding penetrations such as at ventilation ducts, pipes or windows. Thus at each story, water may enter to the drainage system located behind the cladding through the cladding or through deficiencies at through-wall penetrations.

[15] Laws, J. O. and Parsons, D. A. (1943) The relation of raindrop size to intensity, Trans. Amer. Geophysical Union, **24**; pp 452-460
[16] Best, A. C. (1950), The size distribution of raindrops, Quarterly Journal of the Royal Meteorological Society, Vol.76 (327); pp. 16–36

The amount of water that might enter, for example, a stucco clad wall assembly, a photo of which is shown in Figure 11, was determined through experimental testing, where a stucco wall assembly was

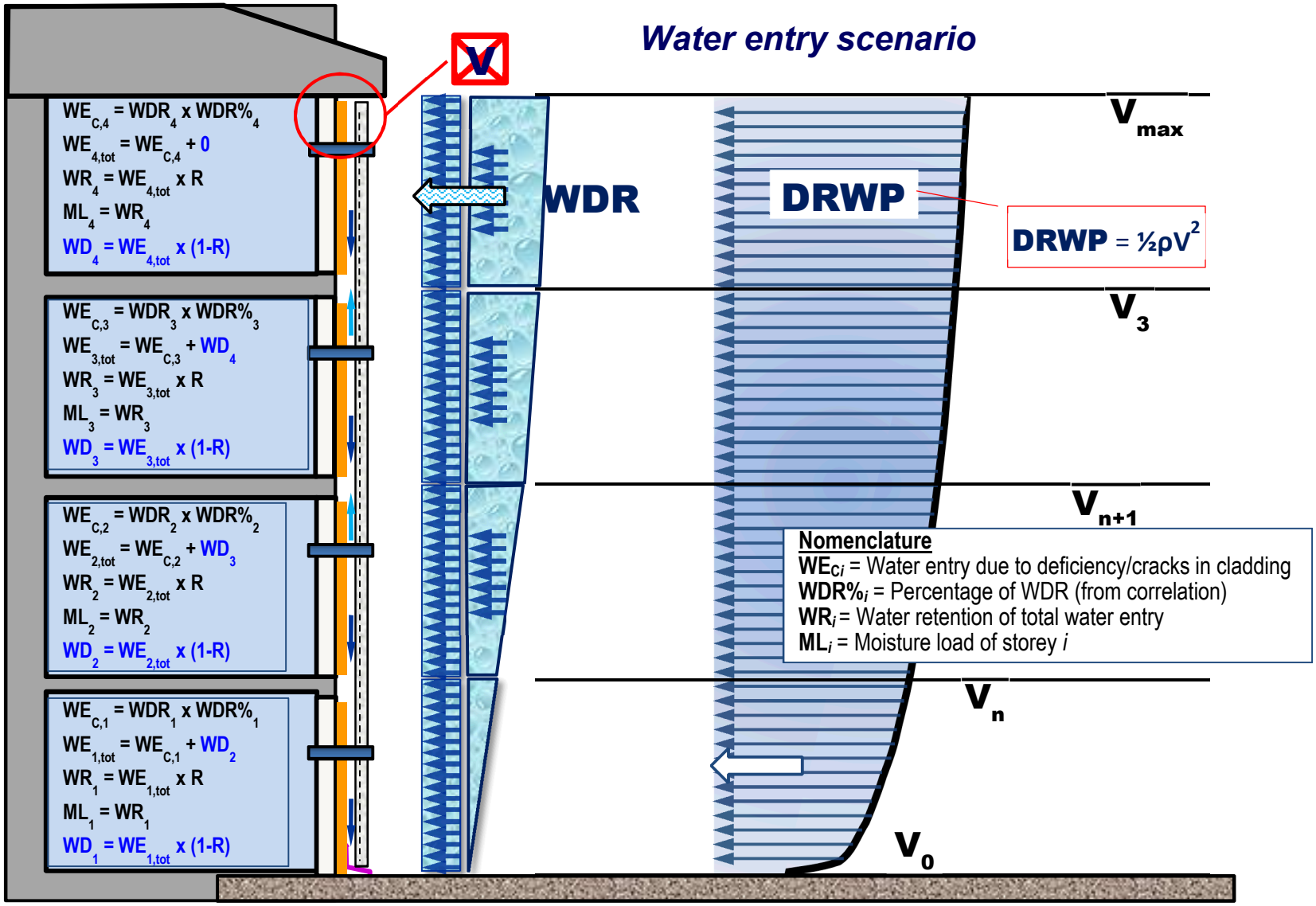

Figure 10 – Schematic illustrating WDR and DRWP loads acting on the cladding to bring about water penetration within and water entry behind the cladding

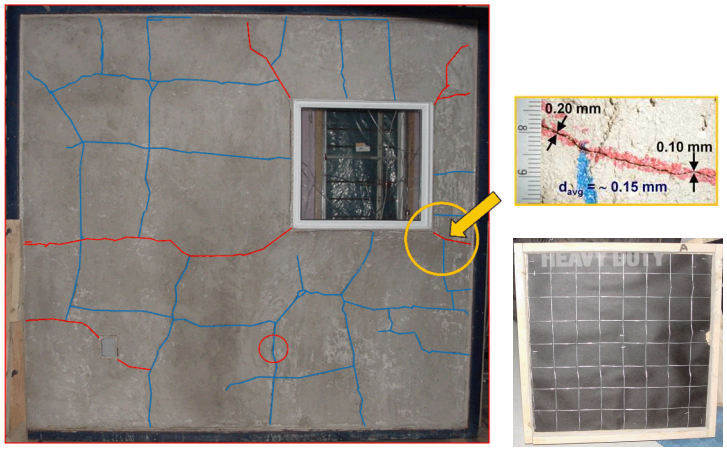

Figure 11 – Stucco cladding subjected to water penetration tests

subjected to varying simulated WDR conditions. This entailed spraying the cladding of a 2.44 m by 2.44 m (8-ft. by 8-ft.) test specimen with water over a range of spray rates whilst simultaneously subjecting the wall to pressure differences. Water that entered cracks and openings in the cladding permeated through it and thereafter was collected to the drainage system over the course of the water penetration test[17].

The percentage of water entry behind a stucco cladding as a function of water deposited on the cladding (L/min-m^2) and pressure difference (Pa) across the wall asembly is provided in Figure 12. A similar set of information was derived for the percentage of water entry at through-wall penetrations and this is likewise shown in Figure 12.

Correlations[18] were developed for low-rise buildings for the percentage of water entry in relation to the water deposition rate (WDR) and pressure difference (P). For water entry behind a stucco cladding, λ, this is given by:

$$\lambda = \left(2.54E-4 \text{ X } 10^{-0.685 \text{ X } WDR} + 6.2E-5\right)P^{1.85}, 0 \leq P \leq 160\ Pa \qquad (12)$$

Whereas, for water entry of deficiencies of through-wall penetrations, ω, such as a ventilation duct, this is given as:

$$\omega = \left(\sum_{i=3}^{3} a_i\, WDR^i\right)\left(b_1 P^{b_2} + c\right), P \leq 150\ Pa, \qquad (13)$$

Where:

ω = Water entry through deficiencies (mL/min);
WDR = Wind driven rain (L/min-m^2), and;
P = Wind pressure (Pa);
And for which the values of the coefficients, a_i, b_i, and c in Eq. (13) are given in Table 5.

[17] Details regarding water penetration testing is given in the Task 5 Report Characterization of Water Entry (see Appendix 1)

[18] A comparison between calculated values for water entry, using the correlations, and those measured, as obtained from testing a stucco-clad wall assembly or of deficiencies of through-wall penetrations is provided in Appx. 3.

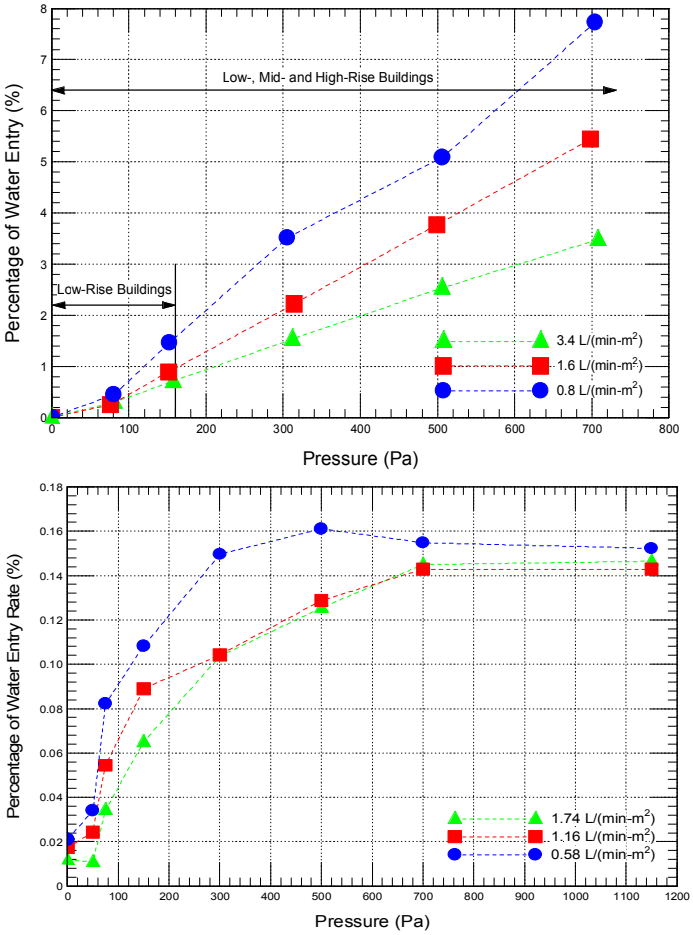

Table 5 – Water entry correlation at deficiencies - Values of correlation coefficients for Eq. 4

Coefficients	P ≤ 150 Pa
a_1	5.66376E-01
a_2	6.38328E-02
a_3	-1.31473E-01
b_1	2.82601E-01
b_2	7.21125E-01
c	9.56514E-01

Figure 12 – Water entry correlations for entry from (i) permeation of stucco cladding and (ii) deficiencies at through-wall penetrations

3.4.3 Water retention in respective drainage systems

Tests were also carried out to characterise the drainage-retention of each drainage system. The depths of drainage cavities for all the drainage system were first determined from the construction of stucco clad mock-ups in accordance with the respective specifications of each of the wall assemblies as provided in the Task 1 Report (see Appendix 1) to which NBC-compliant stucco was applied. The work was undertaken by professedly knowledgeable and experienced stucco contractors. After curing for 28 days, the specimens were then cut at the centre vertically and horizontally so that the interior gaps could be measured to estimate the cavity depth, as seen in Figure 13.

The results provided in Table 6 show the nominal cavity depth, the cavity derived from measurement of the digitized profile of the cavity and the cavity depth used in the numerical simulations and for the fabrication of drainage-retention test specimens. In instances where the measured depth was larger than the nominal depth, the nominal cavity depth was used in the numerical simulations and for the fabrication of drainage-retention test specimens.

Figure 13 – Samples for Drainage Gap Analysis; lines on specimens show locations where specimens were sectioned horizontally and vertically

Table 6 –Summary of Results Obtained for Depths of Venting and Drainage Cavities

NRC Client #	Nominal Cavity Depth mm	Cavity Depth Stucco Applied Mm	Cavity Depth for Simulation mm
Benchmark	10	7	7
Client A	2	2	2
Client B	89	75	75
Client C	10.5	16	10.5
Client D	2	2	2
Client E	10.6	15	10.6
Client F	25	25	25
Client G	9.3	12	9.3
Client H	51	51	51
Client I	3.8	8	3.8
Client J	9.5	-	5.5
Client K	19.5	-	15.5

* Distance between sheathing membrane and inboard of stucco cladding

After determining the cavity depths for each wall configuration, test specimens were constructed to determine the drainage and retention characteristics of each drainage system. The drainage system was that previously described in §3.1.2 and as provided in Table 2.

The 1220 mm wide by 1830 mm high (4ft by 6ft) test specimens were dosed with water to the drainage cavity along the entire width (i.e. 1220 mm) and at constant rates of 3, 4, 5, 6 and 8L/hour for a duration of one hour. The dosage levels were determined from maximum water entry rates that could occur in selected Canadian locations as provided in the Task 5 Report on climate loads (Appendix 1). The quantities of water that drained from the system were monitored gravimetrically during the test, and were used to determine the retention rate of the drainage system. The drainage-retention relation was based on the percentage of water that remained in the cavity for a given water entry rate given in mL/h-m^2.

The results of the drainage-retention tests[19] for all drainage systems evaluated are shown in Figure 14. The results show that a smaller proportion of water is retained for higher dosage rates deposited in the drainage cavity, whereas a greater proportion is retained for lower dosage rates.

[19] The retention characteristics of the respective drainage systems are given in Appendix 4 of the Task 5 report on Characterization of Water Entry, Retention and Drainage of Components; see Appendix 1.

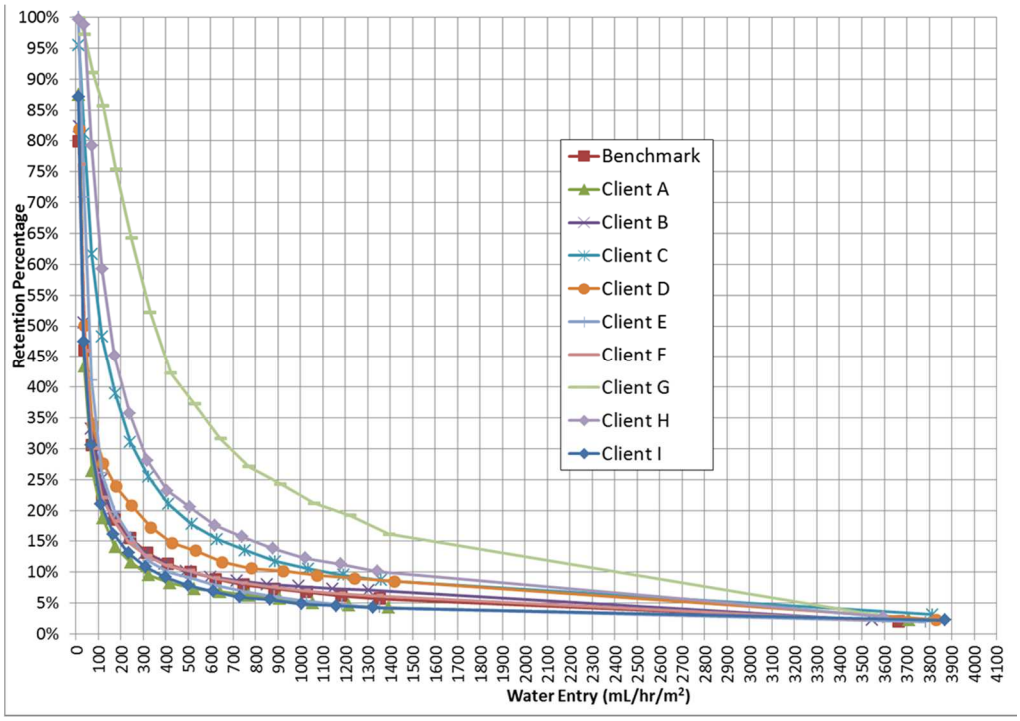

Figure 14 – Driange-retention test results for reference and all Client drainage systems

3.4.4 Moisture loads in drainage cavity at given storey heights

Having determined the water entry rates to the drainage systems on the basis of correlations developed for WDR rain loads acting on the cladding and having assessed the quantity of moisture that might drain from a cavity given the dosage to the cavity, the moisture load within the cavity was then estimated for each storey level.

Referring to the schematic provided in Figure 10, and taking into consideration the WDR loads as provided from Eq.2 and the percentage of these loads that enter the cavity of the drainage system as provided from both Eq. 3 and Eq. 4, the moisture load (ML) at any given story height, *i*, is given by:

$ML_i = WR_i$ (14)

Where:

ML_i = Moisture load of storey *i*
WR_i = Water retention of overall water entry at storey *i* = $WE_{i,tot}$ x R (15)

And where:

R = % retained in the drainage system and 1-R = % water drained from system

$WE_{i,tot}$ = total quantity of water entry at storey *i* = $WE_{C,i} + WD_{i+1}$ (16)

WD_i = Water drainage from the storey above = $WE_{i,tot}$ x (1-R) (17)

$WE_{C,i}$ = Water entry through cladding and from deficiencies to the drainage system

Also:

$$WE_{C,i} = WDR_i \times WDR\%_i \quad (18)$$

$WDR\%_i$ = Percentage of WDR (from correlations given in Eq. 3 and Eq. 4)

WDR_i = Wind-driven rain load at story *i* (as given by Eq. 2)

The moisture loads within the drainage cavity for each storey height are shown in Figure 10. It follows from this that the ML at the fourth storey differs from that of the other three storeys given that the total quantity of water entry at this storey is:

$$WE_{4,tot} = WE_{C,4} + 0 \quad (19)$$

Where in Eq. 10, that portion of water that drains from the storey above, $WD_i = 0$ and as such, the total quantity of water entry to the drainage system at this storey is simply the percentage of WDR that enters from permeation of water through the cladding and through deficiencies, as provided in in Eq. 3 and Eq. 4.

3.4.5 Distribution of moisture loads within drainage cavity

The manner in which moisture loads within a cavity were distributed depended on the presence of a nominal capillary break, as might be assumed for those drainage systems having cavity depths of at least 10 mm, as illustrated in Figure 15.

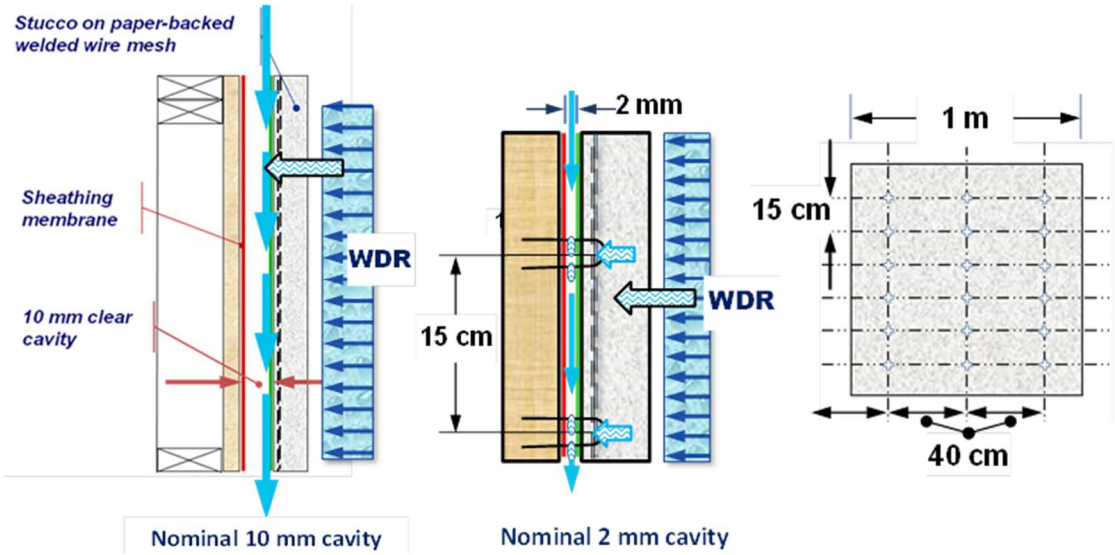

Figure 15 - Distribution of moisture loads within drainage cavities: (a) for cavities having a nominal 10 mm depth; (ii) for cavities of nominal 2-4 mm depth

In these instances, the ML was applied to the backside of the cladding if there was a clear cavity, or when the drainage cavity included a drainage component, it was assumed that 50 % of the ML remained on the backside of the cladding whereas the remaining 50% found its way to the surface of the sheathing membrane. It was surmised that in the case of a clear cavity, the capillary break would prevent any substantial ML from reaching the sheathing membrane, whereas in the presence of a drainage component, it was supposed that there was an equal risk that the ML would remain on the backside of the cladding, or percolate to the surface of sheathing membrane over a storey height.

In instances where the nominal drainage system cavity depth was 2 to 4 mm in depth (Figure 15; ii), it was assumed that all of the ML reached the sheathing membrane. This was deemed a plausible scenario

given that any water that would permeate the cladding would find its way to the drainage space at fastener locations and thus quickly occlude the interstitial space of these drainage systems given the number and schedule of fasteners used to secure stucco cladding to the frame, as illustrated in Figure 15 (ii).

3.4.6 Other assumptions in respect to undertaking of hygrothermal simulations

Initial Conditions

The initial temperature in all layers of the wall assemblies were taken equal to 21°C and the initial moisture content of all material layers corresponded to a relative humidity of 50%. Simulations were started on the first day of the month of January of the average climate year for the specified locations.

4.0 Defining Performance Attributes

Information in this section describes how performance attributes of specific components of the wall assembly were defined and how the performance of the code compliant reference wall was assessed in relation to the client wall assemblies incorporating drainage components. The locations that were of interest in assessing the performance of wall assemblies are defined.

4.1 Locations of interest in assessing performance of wall assemblies

Within the wall assembly there are locations that are of interest given that these may be prone to moisture uptake. Given sufficient temperature conditions and an adequate gestation period, this may lead to the risk of formation of mould or, in the case of wood-based components, wood rot fungi. These locations have been identified in Figure 16. In this figure, a schematic of a vertical sectional view of the reference wall assembly is given with a portion expanded to better illustrate the different layers within the assembly. The layers include the sheathing membrane, the sheathing panel (OSB), and the insulation within the stud cavity of the wall. Focus is placed at these locations, as it is at these locations that the risk to the formation of mould or wood rot is heightened given their proximity to the sheathing membrane and drainage cavity where the moisture loads have been applied.

Accordingly, emphasis has been placed on determining the local temperature and relative humidity conditions, which result from simulating the response of the wall assembly to selected climates, at the following four (4) locations in the wall section:

- Interface between the exterior surface of the sheathing panel (OSB/gypsum board) and cavity
- Exterior portion of sheathing panel of depth 1 mm
- 10 mm portion of sheathing panel (remaining portion of 11 mm panel)
- Interface between the interior surface of the sheathing panel (OSB/gypsum board) and fibrous insulation.

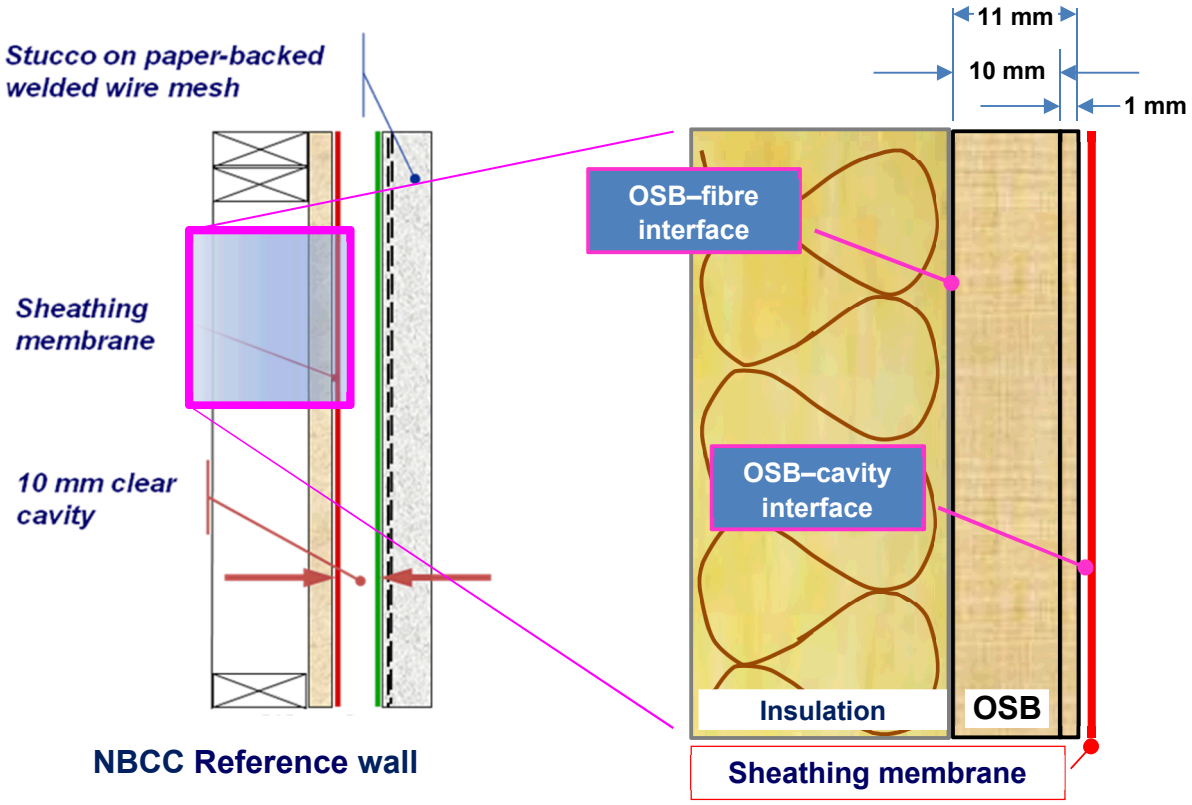

Figure 16 – Locations of interest within wall assemblies in assessing relative performance

4.2 Performance criteria

Two (2) performance criteria were used to assess the performance of wall assemblies. These include the: (i) RHT index, as was used previously in other projects for which the performance of wall assemblies was sought [14], and; (ii) the Mould Index developed by Hukka and Viitanen [[20]], Viitanen and Ojanen [[21], 60] and Ojanen et al. [[22]]. Each of these criteria is described in turn.

4.2.1 RHT index

The RHT index is a measure of the risk of formation of mould on surfaces or wood rot of wood-based components given the relative humidity and tempeature profile over a specified time period over which the index is used. The value of the index increases monotonically and thus represents at the end of the period, the maximum cumulative value of the index. The value of the index is given by the following relation:

$$RHT(x) = \sum_{i=1}^{n}[RH - RH(x)][T - T(y)] \qquad (20)$$

Where:

$RHT(x)$ = Cumulative value of the RHT index

$RH(x)$ = User defined threshold value for relative humidity (RH)

$T(y)$ = User defined threshold value for temperature, T (= 5°C)

n = total number of 10 day intervals over a simulation period (= 37 / 1 year)

If the user defined threshold value for temperature is 5°C, then the value of the index, as given by Eq. 20, accumulates only when the temperature exceeds 5°C, and when the value of RH is likewise above a given threshold value, as is shown in Figure 17.

User defined threshold values for relative humidity % have in previous work been chosen at 80, 90, 92 and 95, depending on the requirements. For example, one might have interest in gaining insight on whether the wood-based components are at risk to attaining critical moisture content where wood rot may be initiated. The relative humidity threshold typically associated with critical moisture content for wood is 97 % RH. Thus $RH(97)$ would be the user defined threshold value for RH when determining values for RTH (97) index.

In this project, values were generated for RHT indices of RHT(80), RHT(85) and RHT(92).

[20] Hukka, A., and Viitanen, H. A. (1999), A mathematical model of mould growth on wooden material, Wood Science and Technology, Volume 33, Issue 6, pp 475-485

[21] Viitanen and Ojanen (2007), Improved Model to Predict Mold Growth in Building Materials, Proceedings of the Buildings X International Conference on the Thermal Performance of the Exterior Envelopes of Whole Buildings (December 2-7), Clearwater Beach, Florida, 8 p.

[22] Ojanen, T., Viitanen, H.A., Peuhkuri, R, Lähdesmäki, K., Vinha, J., and Salminen, K., "Mold Growth Modeling of Building Structures Using Sensitivity Classes of Materials", 11th Itnl. Conference on Thermal Performance of the Exterior Envelopes of Whole Buildings XI (Clearwater, (FL), USA, December-05-10), 10 p., 2010.

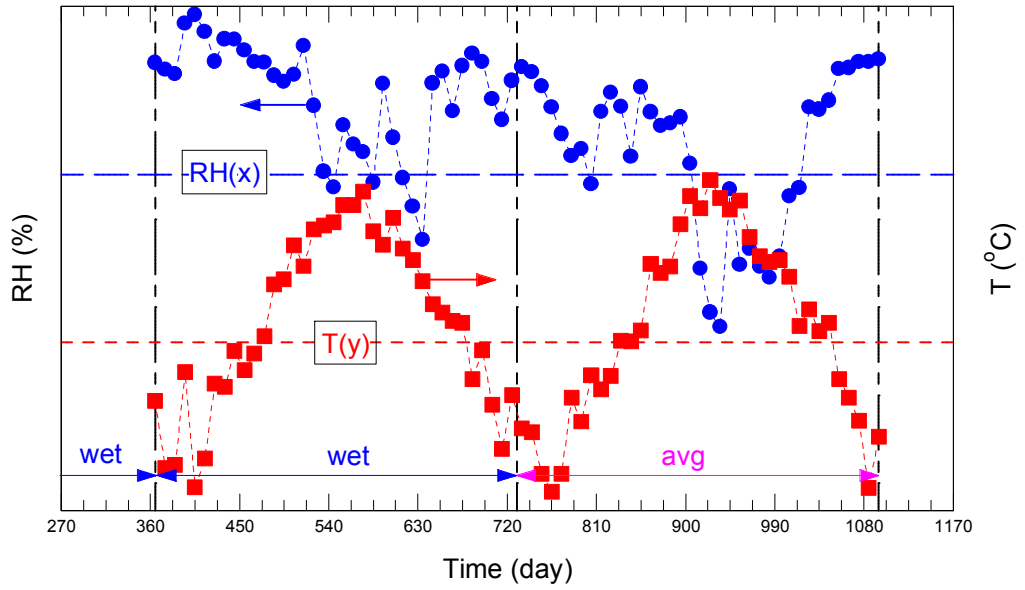

Figure 17 – Relatrive humidity (RH %) and tempeature (T°C) data averaged every 10 days over a 2 year period and representative of simulation conditions

4.2.2 Mould index

The development of the mould index has been on-going for several years with the most recent work, as was used in this project, having being provided by Ojanen et al. [20].

A description of the mould index levels as relate to growth rates is provided Table 7, whereas the mould growth sensitivity classes for specified materials and corresponding minimum levels of relative humidity needed for mould growth are provided in Table 8. The mould index levels range in value from 0 to 6, with 0 being equivalent to no growth and 6 indicating 100% coverage of either heavy or tight mould growth. The visual identification of mould growth on surfaces is given an index level value of 3.

As provided in Table 8, the sensitivity of different construction materials to the formation of mould growth was classified in four (4) classes, namely: very sensitive, sensitive, medium resistant and resistant. The assumed correspondence of sensitivity class for materials located within a wall assembly as modelled in this study is given in Table 9. More specifically, the sensitivity class for the sheathing panel (e.g. OSB) was considered “Sensitive”, whereas the sensitivity class of materials in the cavity insulation (i.e. fiber-based insulation) was considered “Medium Resistant”.

In this project, only the “Sensitive” mould growth sensitivity class was considered when comparing the relative performance of the respective wall assemblies; however, information has also been provided on the “Medium Resistant” the response of the components in the wall if these were considered as being of “Medium Resistant” class.

Table 7 - Description of Mould Index (M) levels [18, 19, 20]

M	Mould Index (M) - Description of Growth Rate
0	No growth
1	Small amounts of mould on surface (microscope), initial stages of local growth
2	Several local mould growth colonies on surface (microscope)
3	Visual findings of mould on surface, < 10% coverage, or < 50% coverage of mould (microscope)
4	Visual findings of mould on surface, 10%–50% coverage, or > 50% coverage of mould (microscope)
5	Plenty of growth on surface, > 50% coverage (visual)
6	Heavy and tight growth, coverage about 100%

Table 8 - Mould growth sensitivity classes and some corresponding materials [20]

Sensitivity Class	Materials	RH_{min} (%)*
Very Sensitive	Pine sapwood	80
Sensitive	Glued wooden boards, PUR with paper surface, spruce	80
Medium Resistant	Concrete, aerated and cellular concrete, glass wool, polyester wool	85
Resistant	PUR with polished surface	85

* Minimum relative humidity needed for mould growth

Table 9 - Mould growth sensitivity classes for different materials of wall assemblies

Sensitivity Class	Layers within Wall Assemblies	RH_{min} (%)*
Very Sensitive		80
Sensitive	Top plate, bottom plate, OSB, foam	80
Medium Resistant	Fibre, gypsum, membranes	85
Resistant		85

* Minimum relative humidity needed for mould growth

4.2.3 Comparison of RHT index to Mould index

A comparison between the limits of applicability of the RHT index to that of the mould index for the "sensitive" and "very sensitive" class of materials is shown in Figure 18. The risk to mould growth as determined by the RHT index, is delineated by a rectangular pattern ranging, on the temperature scale, between 5 to 30°C and from 100 % RH down to respective threshold values for the selected RHT (x) index (i.e. RHT(80); RHT(85); RHT(92); RHT(95)). Whereas in the case of the mould index, the area for risk to the formation of mould has been identified in red and in blue in instances where there is no risk to mould growth.

As is perhaps evident, the RHT index most closely matching that of the mould index is RHT(80) and this is not surprising given that the minimum relative humidity needed for mould growth to "sensitive" and "very sensitive" class of materials is 80% RH. There is as well, deceasing degrees of correspondence between the two mould growth risk indices as the RHT(x) index increases with the least equivalence for the RHT(95) index.

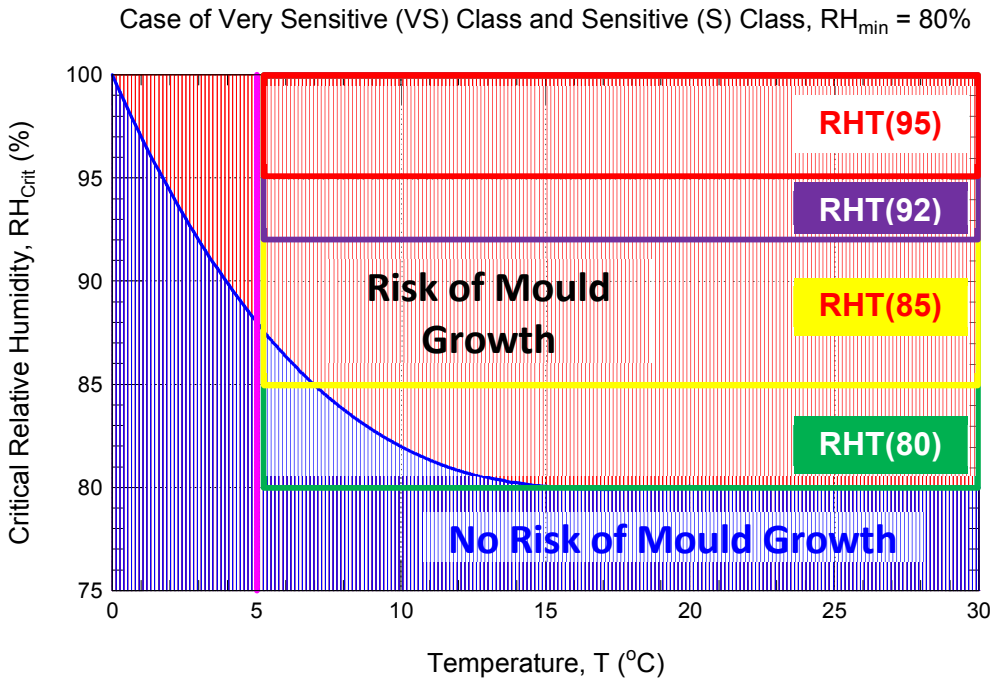

Figure 18 - Comparison between the limits of applicability of the RHT index to that of the Mould index

In this project the performance attributes of the selected locations within the wall assembly were provided at three levels of RHT(x) index (i.e. RHT(80); RHT(85); RHT(92)) and in respect to the mould index, for materials considered as "sensitive" class; an example of this is given in Table 10 and in which both the average and maximum values for the mould index have been provided for the respective locations in the wall as identified in Figure 16.

Table 10 –Mould index values used as performance attributes of wall assemblies

Layer or Interface	OSB Sliver (1 mm thick)	Back OSB (10 mm thick)	Whole OSB (11 mm thick)	OSB-Fibre Interface
Average	3.910	2.506	2.597	1.819
Maximum	4.508	3.475	3.538	2.984

5.0 Results Derived from Hygrothermal Simulation

A comparison of simulation results over 4 storeys is first described, with all subsequent results provided only for the storey for which the response of the wall assembly is the most significant. The comparison is made on the basis of mould index (risk to mould growth) or RHT index (risk to the growth of wood rot fungi).

Thereafter, the results from hygrothermal simulations of the reference wall (Fig. 3) for each of the selected locations in Canada (i.e. Tofino, BC, MI = 3.4; Vancouver, BC, MI = 1.44; and St. John's, NL, MI = 1.41) are provided.

The results provided for the mould index performance are based on a mould index sensitivity class for wood components as "sensitive" (S); the values for RHT index performance are provided for RHT(80), RHT(85), and RHT(95).

5.1 Comparison of simulation results over 4 storeys (Tofino, MI = 3.4)

A comparison of results from simulation of the wall response to local climate loads in three Canadian locations (provided above) and for each of 4 storeys is given in Figure 19 and Table 11. The differences in wall performance as measured by either the mould index or RHT index values for the respective storeys is not clearly evident from the information provided in Figure 19. However, the values for RHT index reported in Table 11 show that the 4th storey is the storey with the greatest value

Figure 19 - Comparison of simulation results over 4 storeys for Tofino, BC (MI = 3.4)

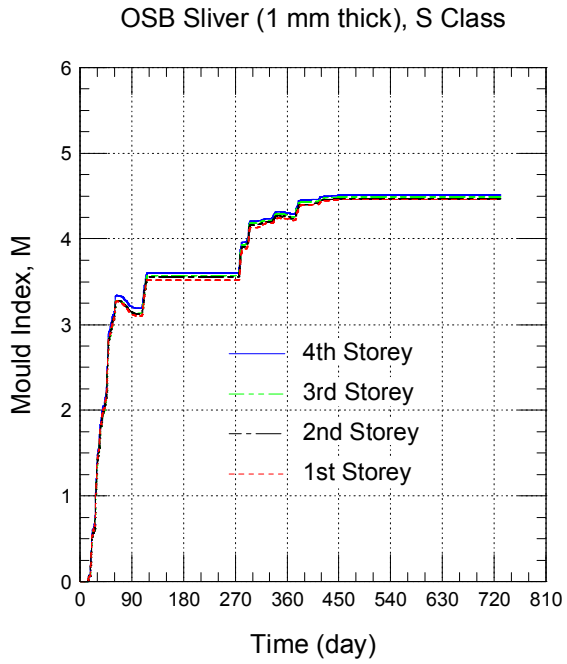

Table 11 – RHT index response of Reference Wall (OSB 1 mm thick sliver)

Storey	RHT(85)	RHT(92)	RHT(95)
4	3015	435	37
3	2972	419	33
2	2912	399	28
1	2864	389	26

Table 12 – Mould index response of Reference Wall (OSB 1 mm thick sliver)

Layer or Interface	OSB Sliver (1 mm thick)	Back OSB (10 mm thick)	Whole OSB (11 mm thick)	OSB-Fibre Interface
Average	3.910	2.506	2.597	1.819
Maximum	4.508	3.475	3.538	2.984

for RHT index. Accordingly, all subsequent values for performance derived from simulation are reported for the fourth and upper-most storey. The corresponding values for the mould index response of a 1 mm

thick sliver of OSB of the 4th storey reference wall are given in Table 12, together with the other values for mould index for other portions of the OSB panel or at its interface with insulation.

5.2 Reference wall simulation - Mould index performance

5.2.1 Comparison in mould index response amongst different locations within wall

The results are first provided with respect to variations in values of mould index for the simulated response of the 4th storey reference wall over a 2-year simulation period (in days) for the specified locations within the wall (i.e. OSB Sliver; Back of OSB; Whole OSB; OSB-Fibre Interface) and in respect to the three (3) locations for which simulation were completed; this is shown for Tofino, BC, in Figure 20, for Vancouver, BC in Figure 21 and in Figure 22 for St. John's, NL.

The values for mould index performance are based on a mould index sensitivity class of wood components of "sensitive" (S). Information in tabular form in the respective inserts provides the average and maximum values of mould index attained for the different locations within the wall section over the 2-year simulation period. As is evident from the information provided in tabular form, the greatest value for mould index performance is attained within the 1 mm sliver located at the exterior extremity of the OSB sheathing panel irrespective of the climate location for which simulations were completed.

Figure 20 – Mould index for specified locations in wall assembly as a function of time over a 2 year simulation period for Tofino, BC

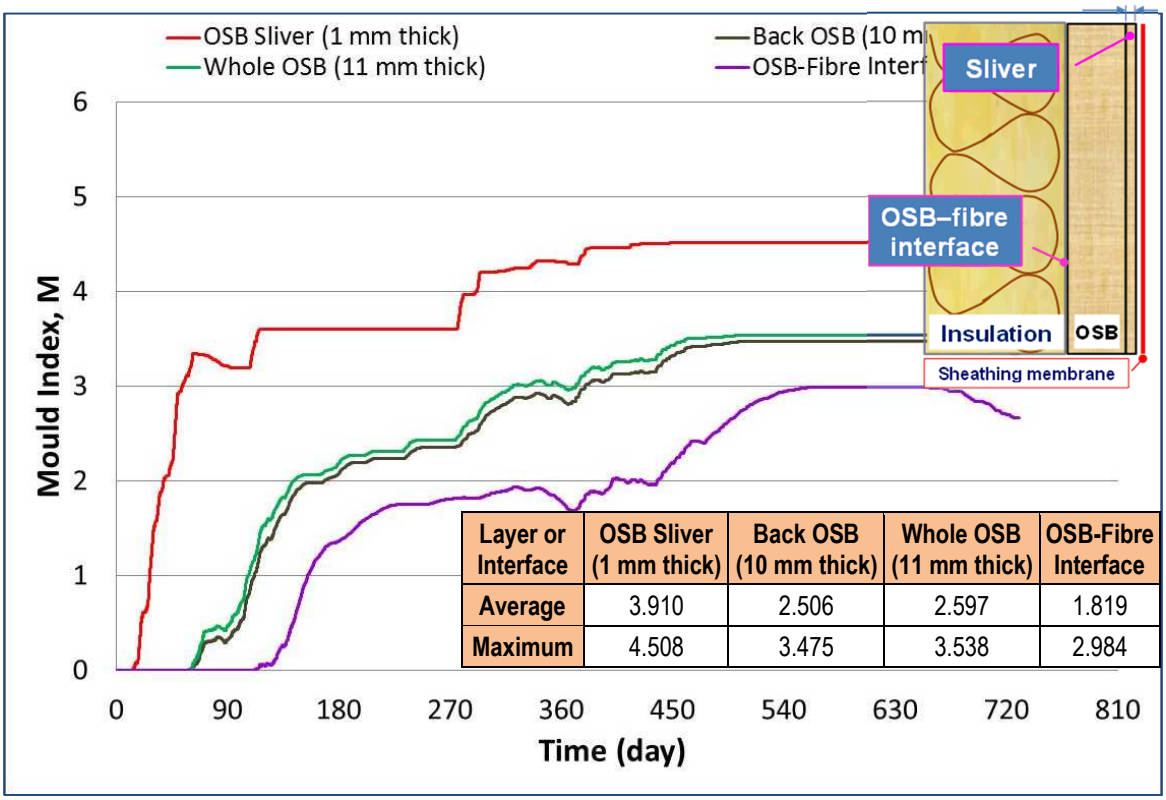

Layer or Interface	OSB Sliver (1 mm thick)	Back OSB (10 mm thick)	Whole OSB (11 mm thick)	OSB-Fibre Interface
Average	3.910	2.506	2.597	1.819
Maximum	4.508	3.475	3.538	2.984

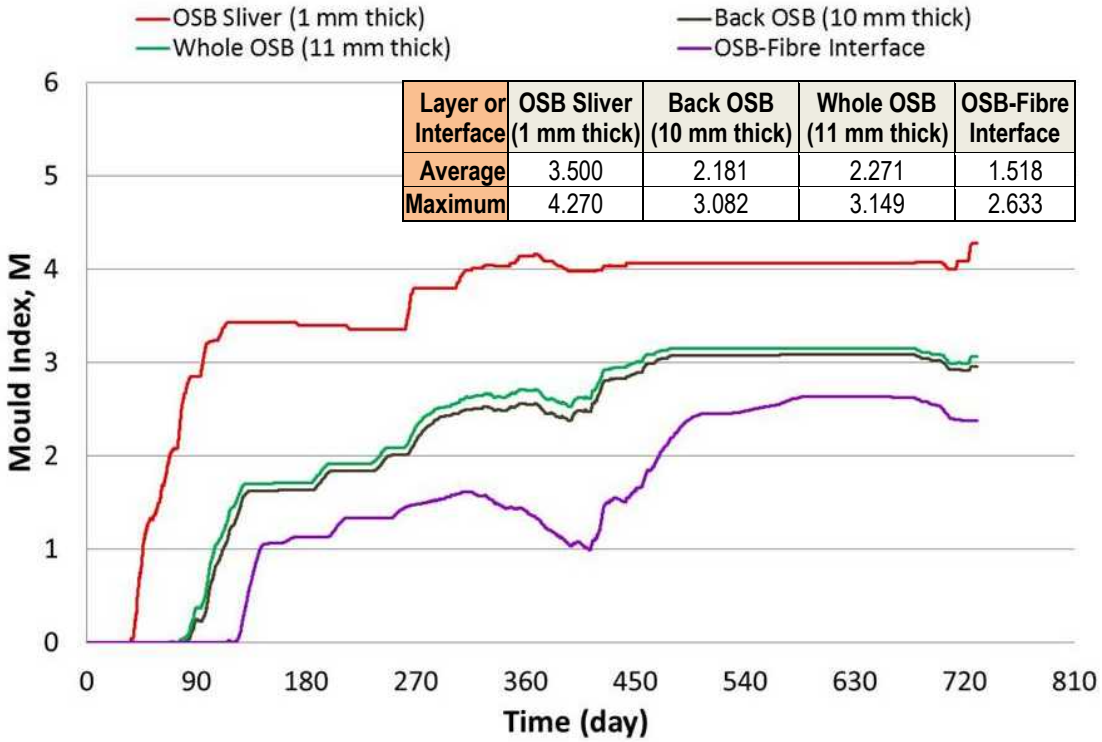

Layer or Interface	OSB Sliver (1 mm thick)	Back OSB (10 mm thick)	Whole OSB (11 mm thick)	OSB-Fibre Interface
Average	3.500	2.181	2.271	1.518
Maximum	4.270	3.082	3.149	2.633

Figure 21 – Mould index for specified locations in wall assembly as a function of time over a 2 year simulation period for Vancouver, BC

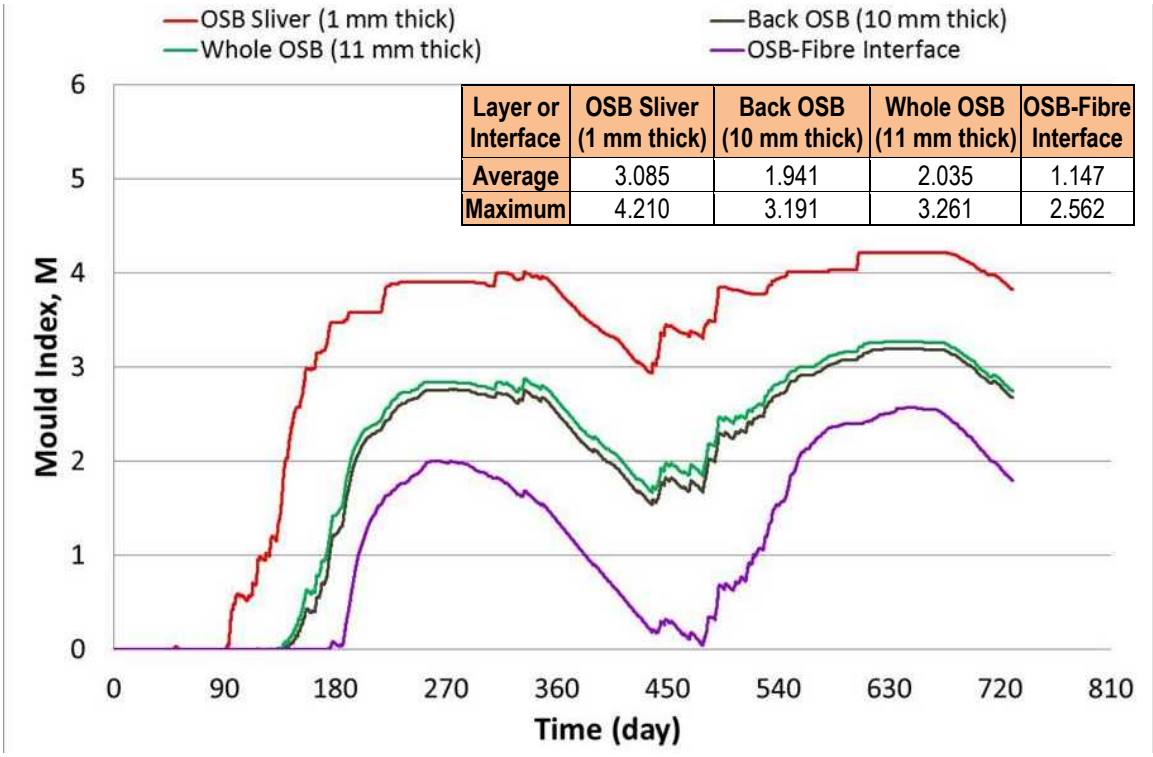

Layer or Interface	OSB Sliver (1 mm thick)	Back OSB (10 mm thick)	Whole OSB (11 mm thick)	OSB-Fibre Interface
Average	3.085	1.941	2.035	1.147
Maximum	4.210	3.191	3.261	2.562

Figure 22 – Mould index for specified locations in wall assembly as a function of time over a 2 year simulation period for St. John's, NL

The average and maximum mould index values for the "OSB sliver" were greatest in Tofino (i.e. $\bar{M}_{IDX}$ = 3.9; max (M_{IDX}) = 4.5), and thereafter, in descending order, in Vancouver ($\bar{M}_{IDX}$ = 3.5; max (M_{IDX}) = 4.3) and St. John's ($\bar{M}_{IDX}$ = 3.1; max (M_{IDX}) = 4.2). As such, the mould index values correlate with the respective values for Moisture index for each climate location.

Reductions in values for mould index during the 2-year simulation period are less pronounced in milder climates as compared to colder climates. For example, the colder climate of St. John's (HDD = 4800) offers significant reductions in mould index values (Sliver: M_{IDX} = 4 to = 3; OSB-fibre interface: M_{IDX} = 2 to = ~ 0.2) over the winter months (i.e. from ca. day 360 to day 450), whereas for the milder climates of Vancouver (HDD = 2950) and Tofino (HDD = 3150), the reductions in M_{IDX} are much less pronounced.

5.2.2 Comparison in mould index response within wall for selected climate locations

The results derived from hygrothermal simulation of the 4th-storey reference wall (Figure 23) for each of three selected locations in Canada over a 2-year simulation period (in days) with respect to the mould index performance values are provided for the 1 mm thick sliver of the OSB sheathing panel in Figure 24, the back of the OSB panel in Figure 25, the "whole OSB panel in Figure 26, and in Figure 27, the interface between the OSB panel and fibrous insulation (see Figure 23).

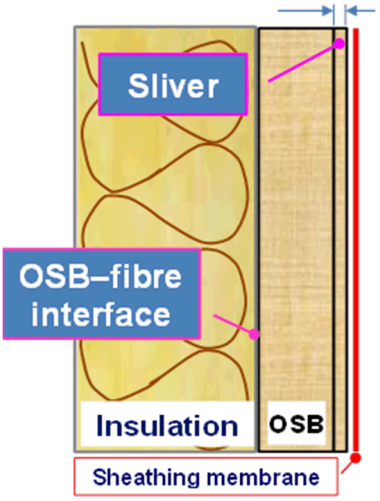

Figure 23 – Locations in wall section of M_{IDX} values

Mould index values for 1 mm "Sliver" (Figure 24)

The mould index values for 1 mm "Sliver" at exterior face of OSB panel of a 4th-storey wall located in Tofino, generally increases over the simulation period, although there is a long period in the initial simulation year where the value of M_{IDX} remains stagnant at a value of ca. 3.6. The response for Vancouver is similar to Tofino, but less severe. For Vancouver the maximum value for M_{IDX} attained after 2-years of simulation is ca. 4.3 whereas for Tofino it is 4.5. In the case of the simulated response of the reference wall located in St. John's, the colder climate retards the growth of the M_{IDX} and provides for a reduction in the M_{IDX} value with the onset of the second winter period; thereafter, it attains a maximum similar in value to that of obtained for Vancouver.

Mould index for the "Back" 10 mm portion of OSB panel (Figure 25)

The mould index values for the "Back" 10 mm portion of the OSB panel of a wall located in Tofino gradually attains a maximum valve for M_{IDX} over the 2-year simulation period of 3.5; a similar pattern of gradual increase in M_{IDX} is evident for Vancouver, although the maximum for M_{IDX} over the 2-year simulation period is 3. For the colder climate of St. John's, the simulated response of the reference wall again is retarded in the initial simulation months, but does achieve a M_{IDX} value of ca. 2.8 in about the ninth month of simulation, only to be reduced over the coming winter months to values of ca. 1.5; thereafter, there is a steady increase again over the subsequent nine months to attain a maximum of ca. 3.2 for this climate location.

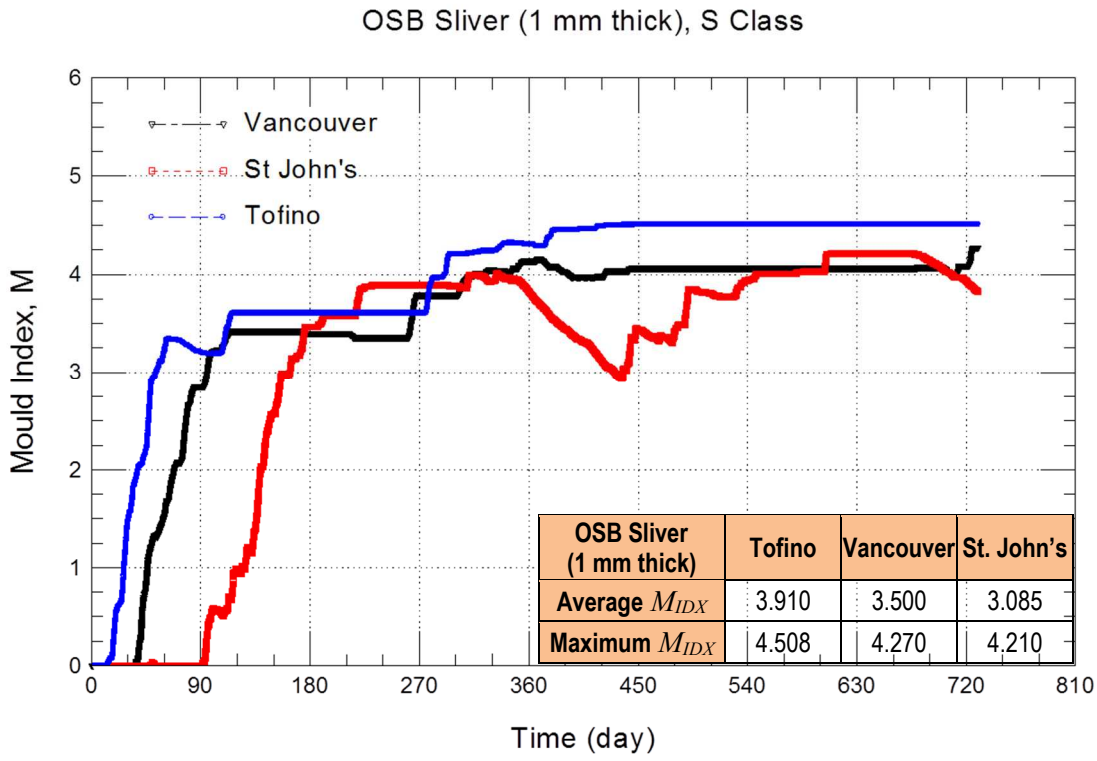

OSB Sliver (1 mm thick)	Tofino	Vancouver	St. John's
Average M_{IDX}	3.910	3.500	3.085
Maximum M_{IDX}	4.508	4.270	4.210

Figure 24 – Mould index for 1 mm "Sliver" at exterior face of OSB panel of a 4th-storey wall for selected climate locations as a function of time over a 2 year simulation period

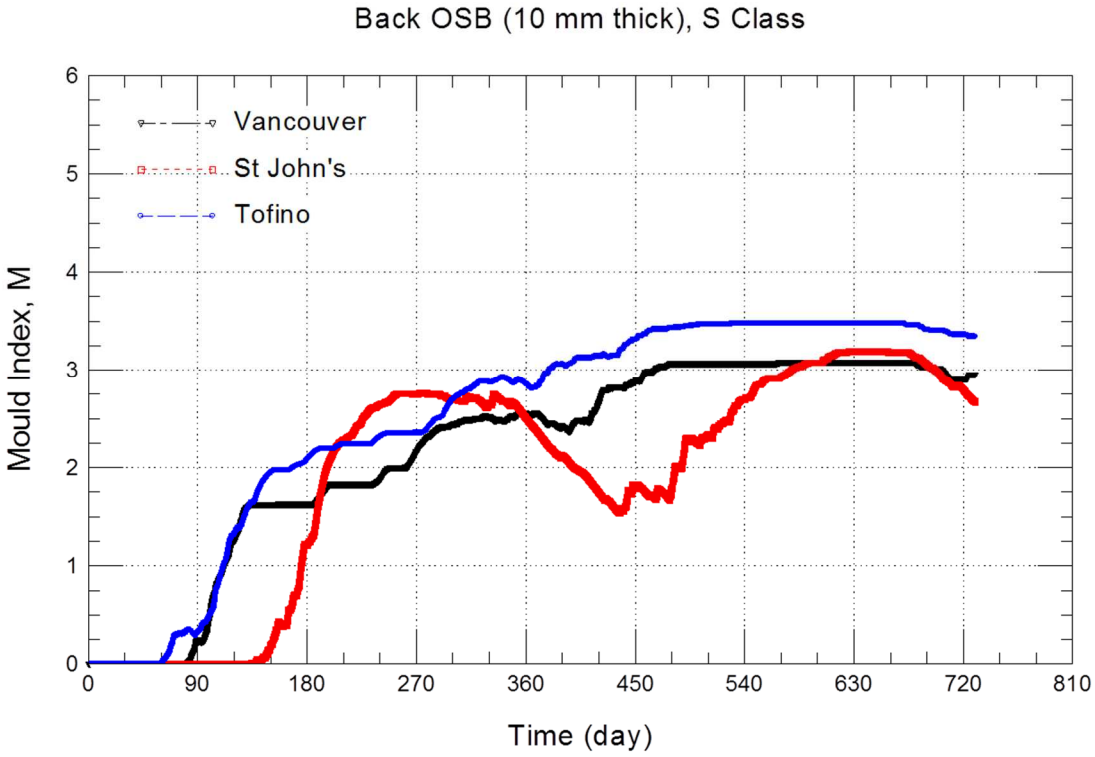

Figure 25– Mould index for the "Back" 10 mm portion of OSB panel of a 4th-storey wall for selected climate locations as a function of time over a 2 year simulation period

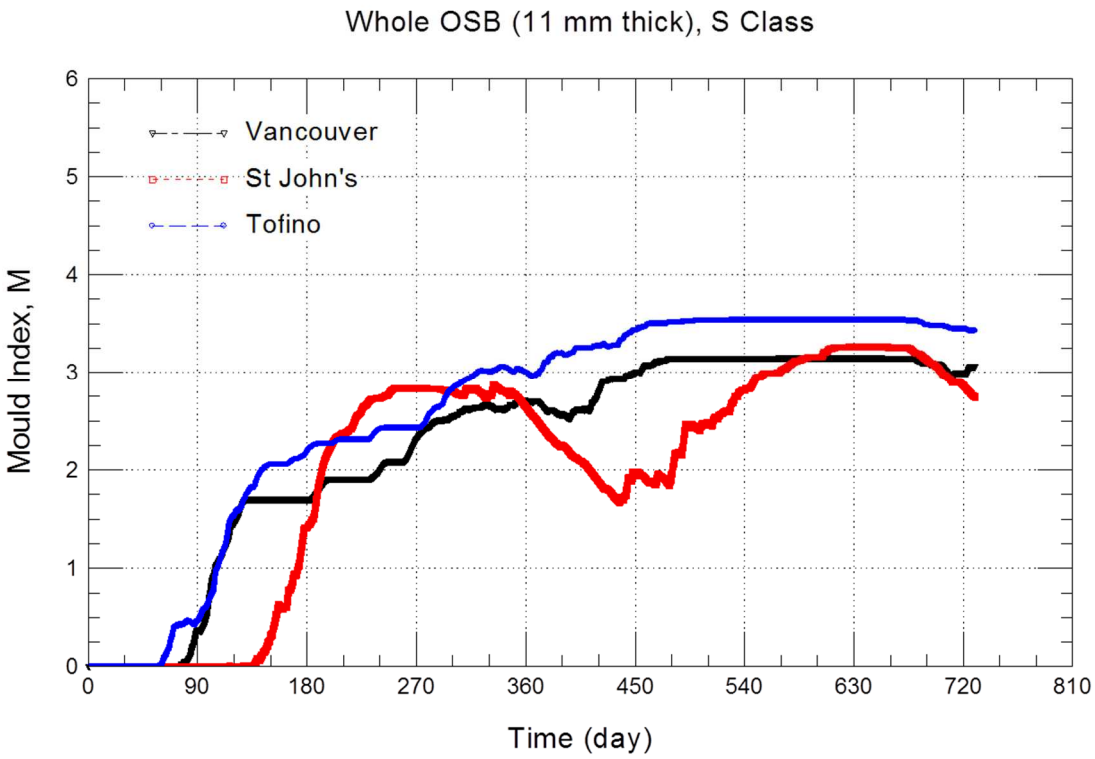

Figure 26 - Mould index for the "Whole" 11 mm portion of OSB panel of a 4th-storey wall for selected climate locations as a function of time over a 2 year simulation period

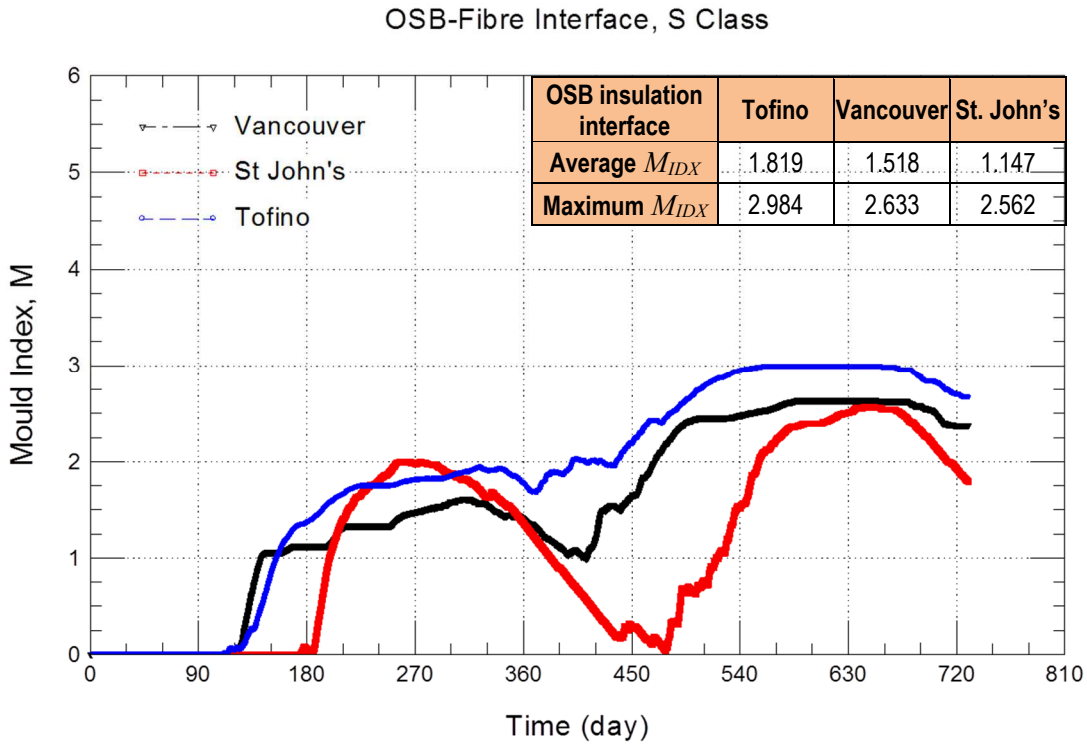

OSB insulation interface	Tofino	Vancouver	St. John's
Average M_{IDX}	1.819	1.518	1.147
Maximum M_{IDX}	2.984	2.633	2.562

Figure 27 - Mould index for interface between OSB panel and fibrous insulation of a 4th-storey wall for selected climate locations as a function of time over a 2 year simulation period

Mould index for the "Whole" 11 mm portion of OSB panel (Figure 26)

The mould index values for the "Whole" 11 mm portion of OSB panel of a wall at the 4th-storey for the selected climate locations is essentially the same as that achieved for the "Back" 10 mm portion of the OSB panel.

Mould index for interface between OSB panel and fibrous insulation(Figure 27)

The mould index values for the interface between the OSB panel and the fibrous insulation within a wall section at the 4th-storey are reduced as compared to the values obtained at the back or for the entire portion of OSB achieving a maximum value for M_{IDX} of ca. 3 for Tofino and ca. 2.6 for either Vancouver or St. John's. This is simply due to lower moisture contents of the OSB at this location in the wall as compared to locations in the OSB closer to the source of the moisture load.

There is a more pronounced effect of the colder seasons on the mould index values as is evident from the lag in accumulation of M_{IDX} values for the initial stages of the simulation and the reduction in M_{IDX} values at the onset of the second as well as the subsequent fall-winter season. Of the three climate locations, this effect is most prominent for St. John's, the coldest of the three climates (i.e. 4800 HDD for St. John's as compared to 3150 and 2950 for Tofino and Vancouver, respectively).

5.2 Results for Reference Wall Simulation - RHT index performance

The results derived from simulation for the response of the 4th storey reference wall subjected to the climate of Tofino over a 2-year simulation period (in days) are shown in Figure 28. In this figure, a relative humidity (% RH) and temperature (°C) plot is provided for the 2-year simulation period for a 1 mm "sliver" of the exterior surface of an OSB panel within a section of the reference wall. The cumulative values for RHT indices achieved after the 2 years simulation are given in the adjoining insert and for which the values for RHT(80), RHT(85), and RHT(92) are provided. The lower the RH threshold value, the higher the value of the corresponding RHT index.

Table 13 – Values of RHT index for Selected climate locations

Tofino (MI = 3.36)		
RHT(80)	RHT(85)	RHT(92)
5263	3015	435

Vancouver (MI = 1.44)		
RHT(80)	RHT(85)	RHT(92)
4958	2493	192

St John's (MI = 1.41)		
RHT(80)	RHT(85)	RHT(92)
2961	1786	193

Similar values have been provided for the respective RHT indices for Tofino (MI = 3.36), Vancouver (MI = 1.44) and St. John's (MI = 1.41) in Table 13. The severity of the Tofino climate is evident from a review of the values for RHT; Tofino has the highest RHT index value for each of the respective indices. As well, it is difficult to distinguish between the severity of the climate in Vancouver and St. John's given that the RHT(92) index value for these locations is essentially the same. However, one is able to obtain more discerning index values from the RHT(85) and RHT(80) indices.

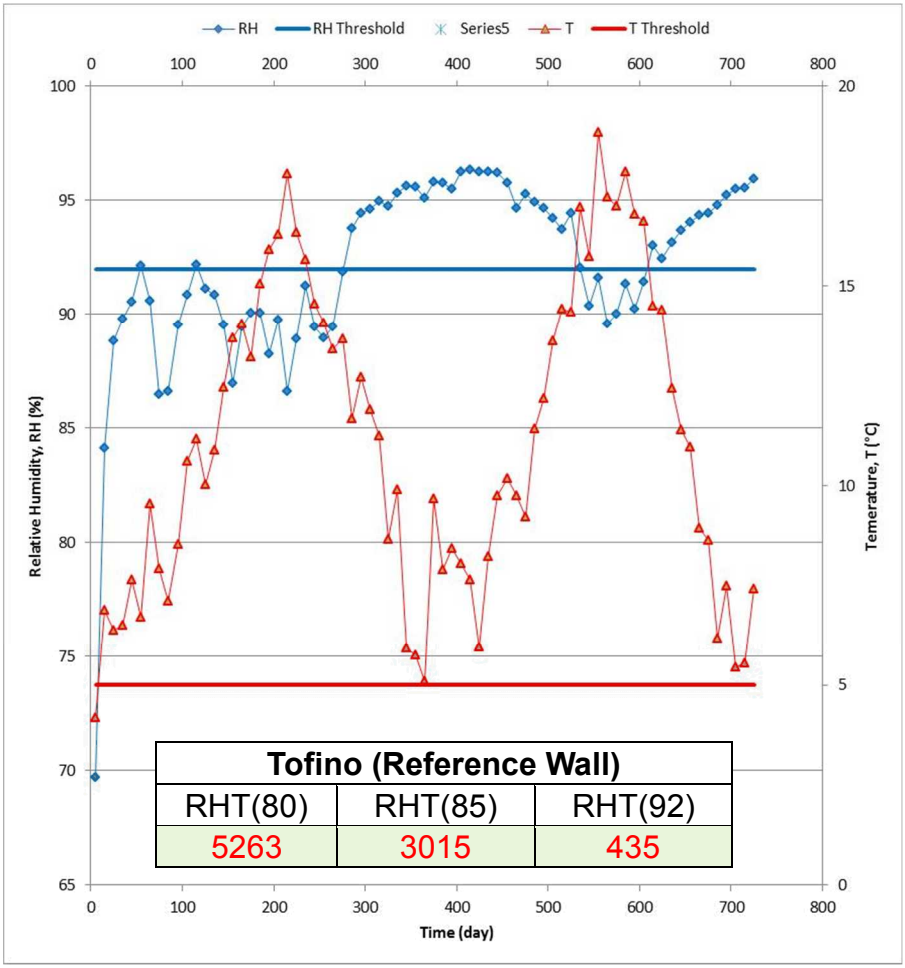

Figure 28 – Relative humidity (%) and temperature (°C) plot over a 2-year simulation period for a 1 mm "sliver" of OSB panel within a section of the reference wall of 4th-storey and subjected to Tofino climate

5.3 Discussion of Simulation Results

The discussion of simulation results focuses on two aspects:

- Trends in response of the reference wall to the three climates to which the walls were subjected
- Location within the section of the wall for which values of M_{IDX} are provided.

Response of the reference wall to different climate locations

The most severe location, based on average and maximum values for M_{IDX}, was Tofino, BC. Average values for M_{IDX} for the OSB panel "sliver" for Tofino were 3.9 as compared to 3.5 for Vancouver and 3.1 for St. John's; values for $\max\{M_{IDX}\}$ for Tofino, Vancouver and St. John's, were respectively, 4.5 (+15%), 4.3 (+23%) and 4.2 (+36%); the values in parentheses provide the % increase from the average values.

This trend is the same for values reported as an RHT index irrespective of whether the index was RHT(80), RHT(85) or RHT(92).

Variation in values of M_{IDX} for location within wall section

In general, for any given climate location, the average and maximum values for M_{IDX} are greatest for locations in the wall assembly closest to the source of the moisture load and decreases as the gap between the moisture source and the location of interest increases. Thus, for example in Tofino, the "sliver" of OSB panel has the greatest average value for M_{IDX} at 3.9, followed by the back portion of the OSB panel (M_{IDX} = 2.5) and thereafter, the interface between the OSB and fibrous insulation (M_{IDX} = 1.8).

The onset for mould growth on or within the OSB panel for any given location is thus more evident for the sliver as compared to the interface between the OSB and fibrous insulation. In Tofino, for example, the onset for mould growth at the 1 mm thick OSB panel "sliver" occurred after the first 15 days whereas this was 120 days for the interface between the OSB and fibrous insulation.

6.0 Conclusions

In this report, information has been provided regarding the inputs required to complete hygrothermal simulations and included the following:

- A summary description of the reference wall assembly
- Description of wall assemblies and their respective drainage component characteristics
- Hygrothermal property characteristics
- Defining climate loads for several Canadian location's including information on the moisture index, annual driving rain index, rainfall, rainfall intensity and prevalent wind-driven rain direction and identification of "average" and "wet" years
- Selection of representative Canadian climate locations for simulation
- Defining the moisture loads acting on components within the wall assembly in consideration of the amount of water entry to and drainage from wall assemblies
- Water retention in drainage systems
- Defining performance attributes of wall components in terms of selected performance criteria including the mould index and RHT index

In addition, a thorough overview of the hygrothermal simulation model hygIRC-C has been provided and as well, examples have been given on exercises undertaken to benchmark the model.

Finally, results from hygrothermal simulation have been presented in which the response of the reference wall to climate conditions of Tofino (BC), Vancouver (BC), and St. John's (NL) have been described. The results, as provided by information on the mould index and RHT index within the assembly, permitted comparisons of the response of the reference wall to the different climates. As such, Tofino was deemed to have the most severe climate of the three locations with the least onerous being St. John's. The colder climate of St. John's was found to attenuate the response of the wall as evident from the reduced values of moisture index for this location as compared to that of either Vancouver or Tofino.

Appendix 1 – List of Task Reports

Report	Reference
Task 1	M. Armstrong and B. Di Lenardo (2014), Performance Evaluation of Proprietary Drainage Components and Sheathing Membranes when Subjected to Climate Loads – Task 1 – Wall Assembly Specifications; Client Report A1-000030.01; National Research Council Canada; Ottawa, ON; 52 pgs.
Task 2	P. Mukhopadhyaya, D. van Reenen and S. Bundalo-Perc (2014), Performance Evaluation of Proprietary Drainage Components and Sheathing Membranes when Subjected to Climate Loads – Task 2 – Building Component Hygrothermal Properties Characterization; Client Report A1-000030.02; National Research Council Canada; Ottawa, ON; 58 pgs.
Task 3	H. H. Saber, W. Maref, and G. Ganapathy, (2015) Performance Evaluation of Proprietary Drainage Components and Sheathing Membranes when Subjected to Climate Loads – Task 3 –Hygrothermal Model Benchmarking; Client Report A1-000030.04; National Research Council Canada; Ottawa, ON; 63 pgs.
Task 4	W. Maref, H. H. Saber and G. Ganapathy (2015), Performance Evaluation of Proprietary Drainage Components and Sheathing Membranes when Subjected to Climate Loads – Task 4 – Characterization of Air Flow within Drainage Cavities; Client Report A1-000030.05; National Research Council Canada; Ottawa, ON; 115 pgs.
Task 5	Steven M. Cornick and Khaled Abdulghani (2013), Performance Evaluation of Proprietary Drainage Components and Sheathing Membranes when Subjected to Climate Loads – Task – Defining Exterior Environmental Loads; Client Report A1-000030.03; National Research Council Canada; Ottawa, ON; 99 pgs.
Task 5	T. Moore and M. A. Lacasse (2015), Performance Evaluation of Proprietary Drainage Components and Sheathing Membranes when Subjected to Climate Loads – Task 5 – Characterization of Water Entry to, Retention and Dissipation from Drainage Components; Client Report A1-000030.06; National Research Council Canada; Ottawa, ON; 43 pgs.
Task 6	H. H. Saber and M. A. Lacasse (2015) Performance Evaluation of Proprietary Drainage Components and Sheathing Membranes when Subjected to Climate Loads – Task 6 – Hygrothermal Performance of NBC-Compliant Reference Walls for Selected Canadian Locations, Client Report A1-000030.07; National Research Council Canada; Ottawa, ON; 59 pgs.
Task 6	H. H. Saber et al. (2015) Performance Evaluation of Proprietary Drainage Components and Sheathing Membranes when Subjected to Climate Loads – Task 6 – Hygrothermal Performance of Wall Assemblies with Cavities or Incorporating Drainage Components for Selected Canadian Locations; Client Report A1-000030.08; National Research Council Canada; Ottawa, ON.
Task 7	M. A. Lacasse (2015) Performance Evaluation of Proprietary Drainage Components and Sheathing Membranes when Subjected to Climate Loads – Task 7 – Summary Report on Experimental and Modelling Tasks and Recommendations; Client Report A1-000030.09; National Research Council Canada; Ottawa, ON.

Appendix 2 – Hourly WDR intensity for selected Canadian locations

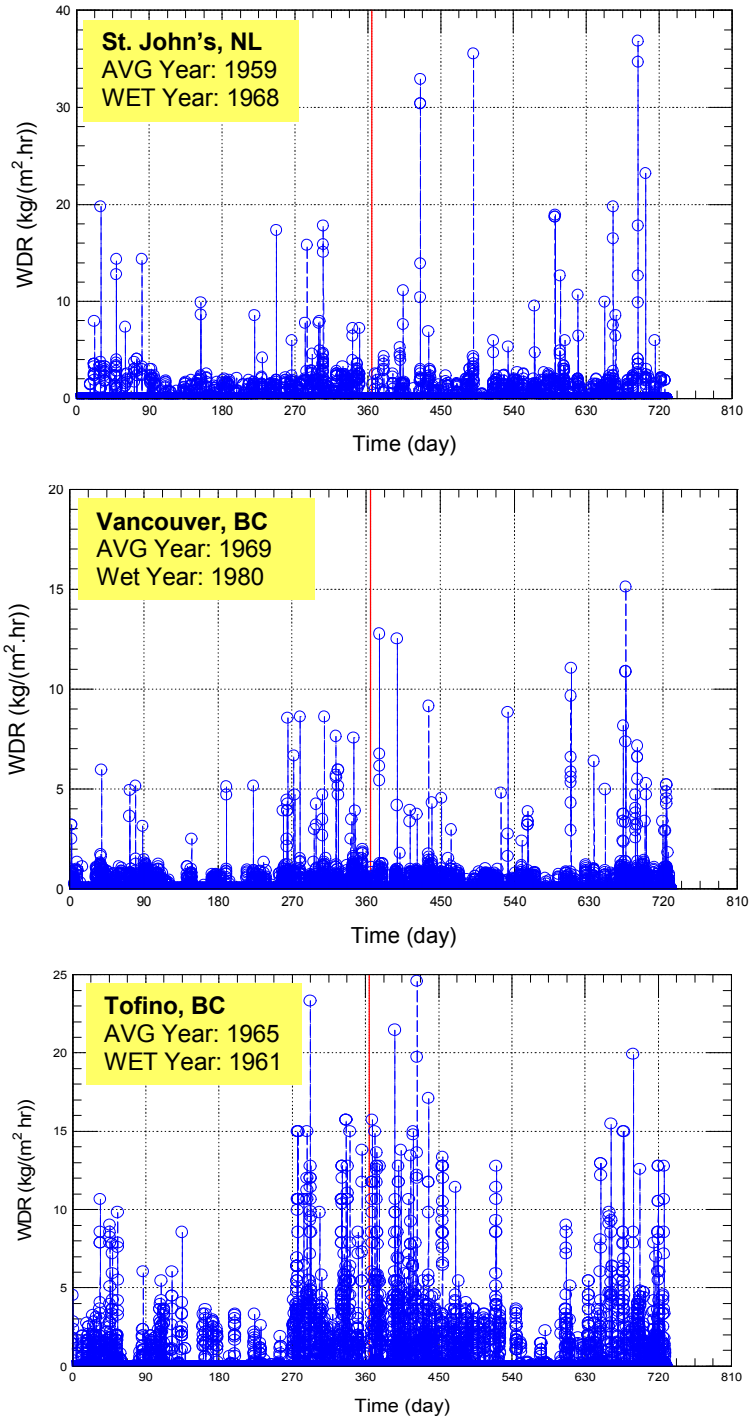

Figure A29 – Hourly WDR intensity for (a) St. John's, NL, (b) Vancouver and (c) Tofino, BC, over an "average" year

Appendix 3 – Water entry correlations - Calculated percentages as compared to measured values

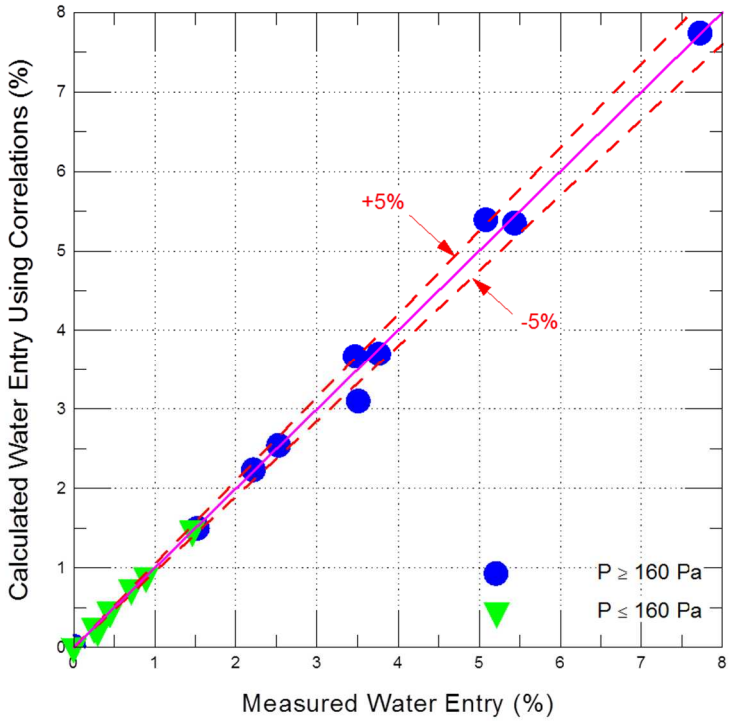

Figure A30 - Correlation for water permeation of a stucco- clad wall assembly

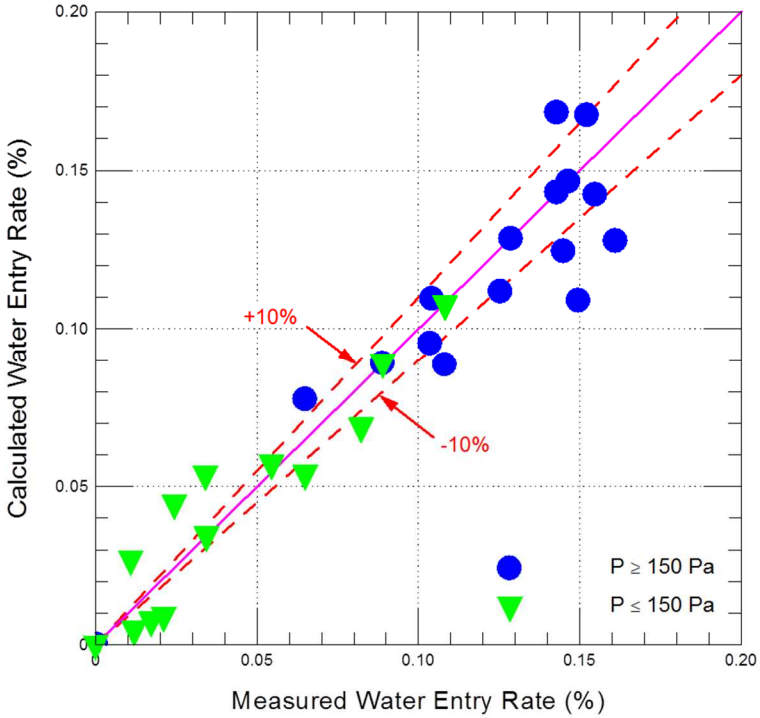

Figure A31- Correlation for water entry at deficiencies of through-wall ventilation duct

Appendix 4 – Simulation results for Reference wall when assuming a Medium Resistant mould growth sensitivity class for wood

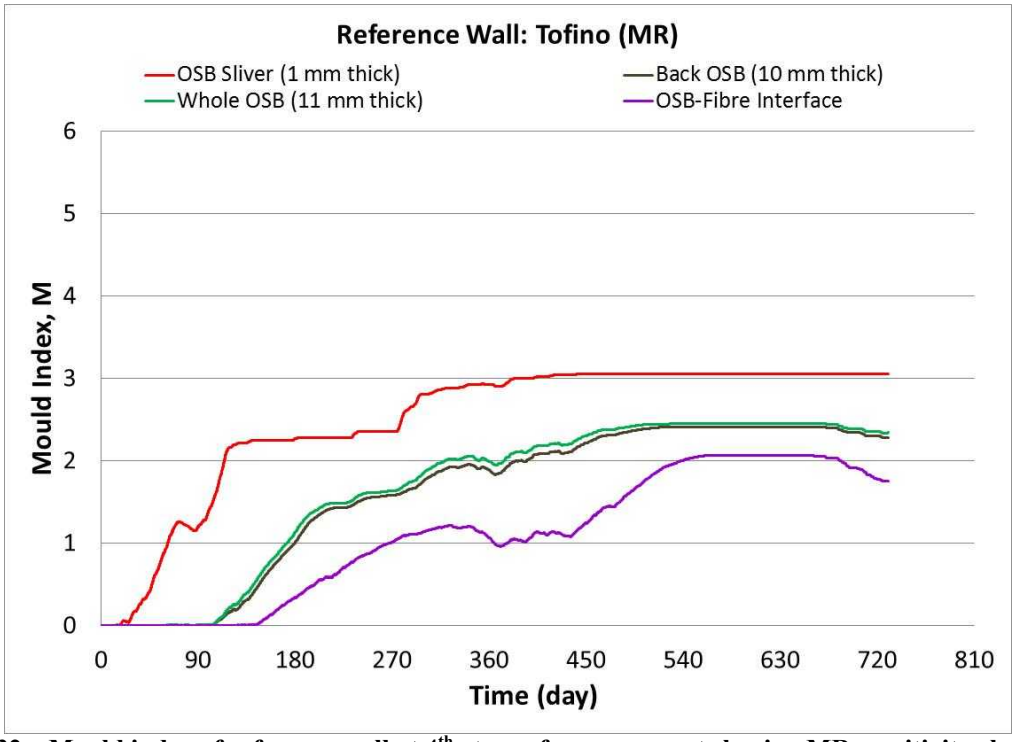

Figure A32 – Mould index of reference wall at 4th-storey for components having MR sensitivity class; Tofino

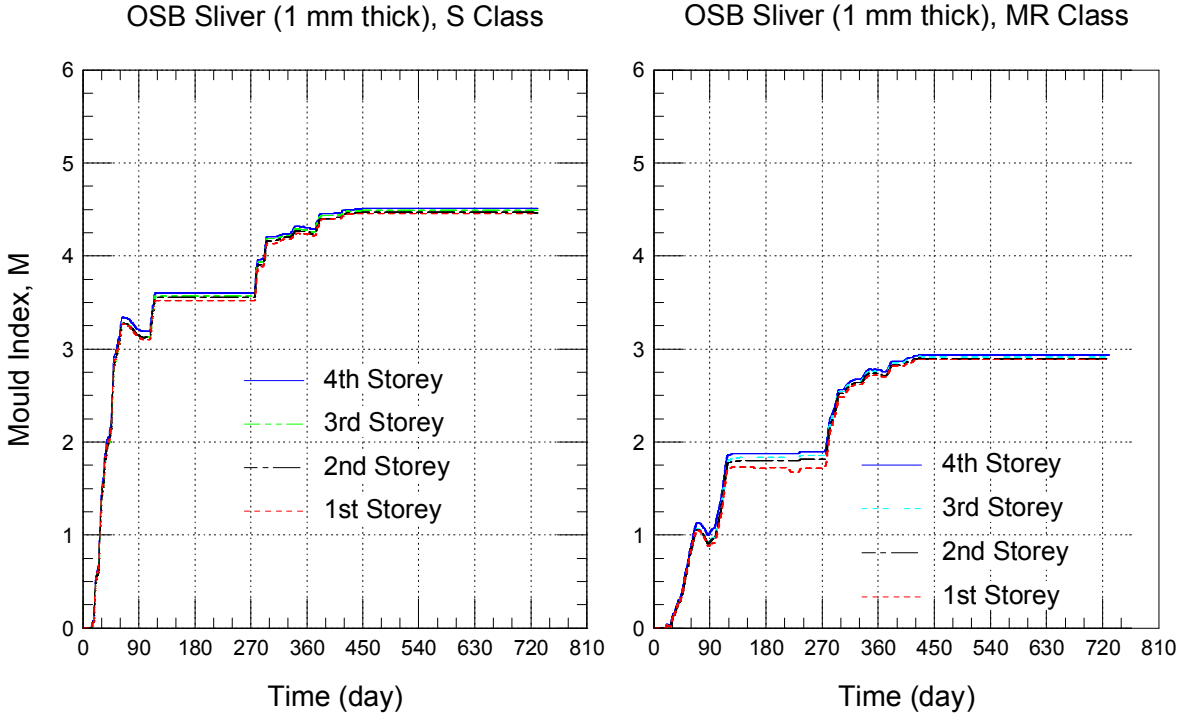

Figure A33 – Mould index values at each storey for components having MR sensitivity class; Tofino